Technical Report
RAL-TR-97-007

String Unification, Spaghetti Diagrams and Infra-Red Fixed Points

B C Allanach and S F King

March 1997

COUNCIL FOR THE CENTRAL LABORATORY OF THE RESEARCH COUNCILS

Enquiries about copyright, reproduction and requests for additional copies of this report should be addressed to:

The Central Laboratory of the Research Councils
Library and Information Services
Rutherford Appleton Laboratory
Chilton
Didcot
Oxfordshire
OX11 0QX
Tel: 01235 445384 Fax: 01235 446403
E-mail library@rl.ac.uk

ISSN 1358-6254

RAL 97-007
SHEP 97-01
hep-ph/9703293

String Unification, Spaghetti Diagrams and Infra-Red Fixed Points

B. C. Allanach[1] and S. F. King[2]

1. Rutherford Appleton Laboratory, Chilton, Didcot, OX11 0QX, U.K.
2. Department of Physics and Astronomy, University of Southampton, Southampton, SO17 1BJ, U.K.

Abstract

We consider a scenario in which the minimal supersymmetric standard model (MSSM) is valid up to an energy scale of $\sim 10^{16}$ GeV, but that above this scale the theory is supplemented by extra vector-like representations of the gauge group, plus a gauged $U(1)_X$ family symmetry. In our approach the extra heavy matter above the scale $\sim 10^{16}$ GeV is used in two different ways: (1) to allow (two-loop) gauge coupling unification at the string scale; (2) to mix with quarks, leptons and Higgs fields via spaghetti diagrams and so lead to phenomenologically acceptable Yukawa textures. We determine the most economical models in which the extra matter can satisfy both constraints simultaneously. We then give a general discussion of the infra-red fixed points of such models, pointing out the conditions for infra-red stability, then discuss two semi-realistic examples: a Higgs mixing model, and a quark mixing model.

1 Introduction

The apparent unification of the gauge couplings at a scale $M_{GUT} \sim 10^{16}$ GeV [1] is an encouraging feature of the MSSM, whose direct experimental verification so far remains out of reach. Nevertheless this conceptual triumph leads naturally to the question of the nature of the new physics *beyond* the MSSM. It is unlikely that the MSSM can survive unchanged above $M_{GUT} \sim 10^{16}$ GeV since the gauge couplings which converge on this scale begin to diverge above it, and are quite unequal at the string scale $M_X \sim 5 \times 10^{17}$ GeV, even taking into account higher Kac-Moody levels and string threshold effects [2]. The traditional approach is to embed the MSSM in some supersymmetric grand unified theory (SUSY GUT) but such an approach presents many theoretical and phenomenological challenges [3, 4, 5], and we shall not consider it further here.

In string gauge unification the three gauge couplings of the MSSM are directly related to each other at the string scale M_X [6]. String theories give the relation [7]

$$M_X = 5.27 \times 10^{17} g_X \text{ GeV}, \tag{1}$$

where g_X is the unified gauge coupling at the string scale M_X. If the MSSM (and nothing else) persists right up to the string scale M_X such theories do not appear to be viable since we know that the gauge couplings cross at $\sim 10^{16}$ GeV, and significantly diverge at the string scale $\sim 5 \times 10^{17}$ GeV. However the situation is in fact not so clear cut since the $U(1)_Y$ hypercharge gauge coupling has an undetermined normalisation factor $k_1 \geq 1$ (where for example $k_1 = 5/3$ is the usual GUT normalisation) which may be set to be a phenomenologically desired value [8] by the choice of a particular string model. However the simplest string theories (e.g. heterotic string with any standard compactification) predict equal gauge couplings for the other two observable sector gauge groups $g_2 = g_3$ at the string scale M_X, which would require a rather large correction in order to account for $\alpha_s(m_Z)$ [7, 9]. In fact, a recent analysis [2, 10] concludes that string threshold effects are insufficient by themselves to resolve the experimental discrepancy. The analysis also concludes that light SUSY thresholds and two-loop corrections cannot resolve the problem, even when acting together. In order to allow the gauge couplings to unify at the string scale it has been suggested [11] that additional heavy exotic matter in vector-like representations should be added to the MSSM at some intermediate scale or scales $M_I < M_X$, leading to the so called MSSM+X models. A detailed unification analysis of such models was performed by Martin and Ramond (MR) [12] for example.

In a previous paper [13] we performed a general unification analysis of MSSM+X models, focusing on the infra-red fixed point properties of the top quark mass prediction, using similar techniques to those proposed for the MSSM and GUTs [14, 15, 16]. The main result was that the top quark mass tends to be heavier than in the MSSM, and closer to its quasi-fixed point in these models. In the present paper we consider a scenario in which the MSSM is valid up to an energy scale of $M_I \sim 10^{16}$ GeV. Above this scale the theory is supplemented by extra vector-like representations of

the gauge group, plus a gauged $U(1)_X$ family symmetry. The basic idea of our approach is that the extra heavy matter above the scale $\sim 10^{16}$ GeV may be used in two different ways: (1) to allow (two-loop) gauge coupling unification at the string scale; (2) to mix with quarks, leptons and Higgs fields via spaghetti diagrams and so lead to phenomenologically acceptable Yukawa textures. We emphasise that in this approach the operators required for Yukawa textures are generated from the dynamics of the effective field theory beneath the string scale rather than from the string theory itself. The overall philosophy of the approach so far is just to explain the data on fermion masses and mixing angles qualitatively. Unfortunately, once the extra fields have been added there are many extra free parameters than data points. It was pointed out by Ross [17] that if there were an infra-red stable fixed point in the renormalisation group flow of these models, it might be possible to constrain all of the parameters of the model at some high scale (but below the string scale). This would make the model quantitative and predictive (and therefore testable). If properly realised, this approach has the potential to predict all of the masses and mixings in terms of about two free parameters. Ross provided an example of such a model with extra heavy Higgs-type multiplets and showed that (under a certain approximation) the model did indeed possess an infra-red stable fixed point. Our work differs from that of Ross [17] in that we perform a detailed analysis of string gauge unification, and in addition we allow more general mixing possibilities along the Higgs, quark and lepton lines of the spaghetti diagrams. In our approach these two questions are related since the extra states required for unification are also used for spaghetti mixing. This economical double use of the extra heavy matter is the main new idea of the present paper. We also give a general discussion of the fixed points of such models, pointing out the conditions for infra-red stability.

The layout of the remainder of this paper is as follows. In section 2 we show how Yukawa textures may be generated from a broken $U(1)_X$ gauged family symmetry where the desired operators are generated from the effective field theory beneath the string scale via spaghetti diagrams. In section 3 we discuss a two-loop analysis of string gauge unification, where the extra states are consistent with the requirements of the previous section. In section 4 we give a general discussion of the infra-red fixed point nature of such models, then discuss two semi-realistic examples. Section 5 concludes the paper. Appendix 1 summarises the running of the gauge couplings to two loops in models with matter additional to the MSSM, appendix 2 lists the wave-function renormalisations for the general model discussed in section 4, appendix 3 details the infra-red fixed point of the Higgs mixing model, and appendix 4 details the infra-red fixed point of a quark-line mixing model.

2 Yukawa Textures from $U(1)_X$ Family Symmetry, Vector Representations and Spaghetti Diagrams

Some time ago, Ibanez and Ross (IR) [18] showed how the introduction of a gauged $U(1)_X$ family symmetry to the MSSM could be used to provide an explanation of successful quark and lepton Yukawa textures. The idea is that the $U(1)_X$ family symmetry only allows the third family to receive a renormalisable Yukawa coupling but when the family symmetry is broken at a scale not far below the string scale other families receive suppressed effective Yukawa couplings. The suppression factors are essentially powers of the vacuum expectation values (VEVs) of θ fields which are MSSM singlets but carry $U(1)_X$ charges and are responsible for breaking the family symmetry. The relevant operators that give the small effective Yukawa couplings are scaled by heavier mass scales M identified as the masses of new heavy vector representations which also carry $U(1)_X$ charges. IR envisaged a series of heavy Higgs doublets of mass M with differing $U(1)_X$ charges which couple to the lighter families via sizable Yukawa couplings that respect the family symmetry. The heavy Higgs doublets also couple to the MSSM Higgs doublets via θ fields and this results in suppressed effective Yukawa couplings when the family symmetry is broken.

More recently Ross [17] has combined the idea of a gauged $U(1)_X$ family symmetry with a previous discussion of infra-red fixed points. The idea behind this approach is that since there are no small Yukawa couplings one may hope to determine all the Yukawa couplings by the use of infra-red fixed points along similar lines to the top quark Yukawa coupling determination. This attractive idea thus allows the determination of otherwise unknown parameters in the model, simply by the dynamics of the renormalisation group (RG) flow of the model. An explicit model was discussed in detail [17], based on the MSSM gauge group enhanced by $U(1)_X$. The question of gauge coupling unification was addressed [17] by adding complete $SU(5)$ $5 \oplus \bar{5}$ representations (which contain the additional Higgs states required for the mixings) to the MSSM theory with masses just below the unification scale. These have no relative effect on the running of the three gauge couplings to one loop order, however at two-loop order it was claimed that the unification scale is raised. However we find that such a mechanism is not completely viable, and we replace it (in the next section) by a general two-loop analysis of the string gauge unification, where the heavy exotic matter has a mass close enough to the string scale to allow it to be also used for the generation of Yukawa textures, as we explain later in this section.

Following IR [18] we introduce a gauged $U(1)_X$ family symmetry into the MSSM. The way this is achieved is well documented and here we only sketch the main results. The quark and lepton multiplets are assigned family dependent (FD) charges as shown in Table 1.

The need to preserve $SU(2)_L$ invariance requires left-handed up and down quarks (leptons) to have the same charge. This, plus the additional requirement of symmetric matrices, indicates that all quarks (leptons) of the same i-th generation transform with the same charge α_i. It is further assumed that quarks and leptons of the same

	Q_i	U_i^c	D_i^c	L_i	E_i^c	H_1	H_2
$U(1)_{FD}$	α_i	α_i	α_i	α_i	α_i	$-2\alpha_3$	$-2\alpha_3$

Table 1: $U(1)_{FD}$ charges assuming symmetric textures.

family have the same charge (this additional assumption was made by Ross [17]). The full anomaly free Abelian group involves an additional family independent component, $U(1)_{FI}$, and with this freedom $U(1)_{FD}$ is made traceless without any loss of generality[1]. Thus we set $\alpha_1 = -(\alpha_2 + \alpha_3)$.

Making the above assumptions all charge and mass matrices have the same structure under the $U(1)_{FD}$ symmetry. The FD charge matrix involving two quark or lepton fields and a Higgs is of the form

$$\begin{pmatrix} -2\alpha_2 - 4\alpha_3 & -3\alpha_3 & -\alpha_2 - 2\alpha_3 \\ -3\alpha_3 & 2(\alpha_2 - \alpha_3) & \alpha_2 - \alpha_3 \\ -\alpha_2 - 2\alpha_3 & \alpha_2 - \alpha_3 & 0 \end{pmatrix} \tag{2}$$

Acceptable textures are obtained for

$$\frac{\alpha_3}{\alpha_2 - \alpha_3} = 1 \tag{3}$$

or

$$\alpha_2 = 2\alpha_3 \tag{4}$$

However these are only the family dependent charges. The total $U(1)_X$ charges are given by

$$U(1)_X = U(1)_{FD} + U(1)_{FI} \tag{5}$$

where

$$U(1)_{FI} \equiv U(1)_T + U(1)_F \tag{6}$$

where the corresponding FI charges are denoted by t, f and the resulting $U(1)_X$ charges are given in Table 2.

	Q_i	U_i^c	D_i^c	L_i	E_i^c	H_1	H_2
$U(1)_X$	$\alpha_i + t$	$\alpha_i + t$	$\alpha_i + f$	$\alpha_i + f$	$\alpha_i + t$	$-2\alpha_3 - (f + t)$	$-2\alpha_3 - 2t$

Table 2: $U(1)_X$ charges assuming symmetric textures.

The choice of FI charges in Table 2 is the most general choice consistent with anomaly cancellation amongst the quarks and leptons via the Green-Schwarz mechanism [18] which is based on assigning $SU(5)$ multiplets equal charges. The Higgs charges are chosen to as to allow a renormalisable coupling to the third family and so the charge matrix in Eq.2 applies equally well to the $U(1)_X$ charges. In order to

[1]Since we assume that the 33 operator is renormalisable, the relaxation of the tracelessness condition does not change the charge matrix since any additional FI charges can always be absorbed into the Higgs charges $H_{1,2}$.

allow anomaly cancellation amongst the Higgs doublets, and permit a renormalisable μ mass term between the Higgs doublets we must arrange that the Higgs carry zero X charge, which in turn implies that the third family has zero X charge, and this is accomplished by choosing:

$$f = t = -\alpha_3, \tag{7}$$

Putting $\alpha_3 = 1$, where the $U(1)_X$ symmetry is broken by the VEVs of MSSM singlet fields θ and $\bar{\theta}$ with $U(1)_X$ charges -1 and +1 respectively implies the following simple X charges for the three families:

$$\begin{array}{ll} 1^{st} \text{ family:} & X = -4 \\ 2^{nd} \text{ family:} & X = +1 \\ 3^{rd} \text{ family:} & X = 0 \end{array} . \tag{8}$$

Since the Higgs charges are zero the charge matrix is simply the matrix given by the sum of the quark (or lepton) charges from each family:

$$\begin{pmatrix} -8 & -3 & -4 \\ -3 & +2 & +1 \\ -4 & +1 & 0 \end{pmatrix} \tag{9}$$

In any mass term, the sum of the charge of the fields in that term must be zero to preserve U(1)$_X$. Thus from Eq.9, the operators that could possibly generate the U quark mass matrix are:

$$\begin{array}{lll} Q_3U_3^cH_2, & Q_3U_2^cH_2(\bar{\theta}), & Q_2U_3^cH_2(\bar{\theta}), \\ Q_2U_2^cH_2(\bar{\theta})^2, & Q_3U_1^cH_2(\theta)^4, & Q_1U_3^cH_2(\theta)^4, \\ Q_1U_1^cH_2(\theta)^8, & Q_2U_1^cH_2(\theta)^3, & Q_1U_2^cH_2(\theta)^3. \end{array} \tag{10}$$

Because each θ or $\bar{\theta}$ field corresponds to a suppression factor of ϵ (where $\epsilon = <\theta> /M_I = <\bar{\theta}> /M_I$) the corresponding texture is of order

$$\begin{pmatrix} \epsilon^8 & \epsilon^3 & \epsilon^4 \\ \epsilon^3 & \epsilon^2 & \epsilon \\ \epsilon^4 & \epsilon & 1 \end{pmatrix}. \tag{11}$$

We now turn to the question of the origin of the non-renormalisable operators in Eq.10. A natural answer to this question was provided early on by Froggatt and Nielsen (FN) [19]. The basic idea involves some new heavy matter of mass[2] M_I which are in vector representations of the MSSM gauge group and which carry charges under the family group $U(1)_X$. The vector-like matter couples to ordinary matter (quarks, leptons, Higgs) via the MSSM singlet fields θ and $\bar{\theta}$ leading to "spaghetti-like" tree-level diagrams. The spaghetti diagrams yield the effective non-renormalisable operators in Eq.10.

[2]We will identify the new heavy matter required to generate the non-renormalisable operators with the new heavy matter required to ensure string gauge unification so we take the mass scale to be M_I.

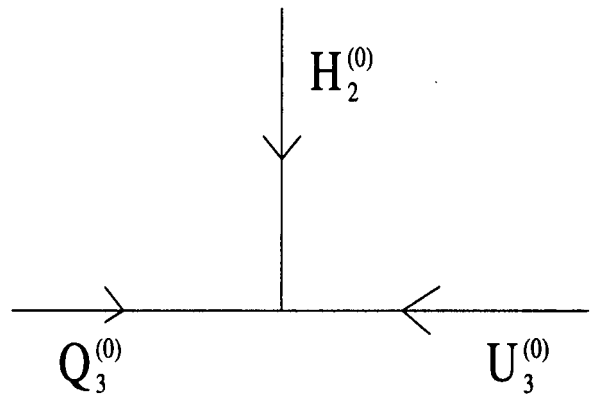

Figure 1: Renormalisable 33 operator.

An explicit realisation of this mechanism was discussed by IR[18] and subsequently by Ross [17], based on the heavy vector-like matter corresponding to additional Higgs doublets which could mix with the MSSM doublets H_1, H_2 via the spaghetti diagrams. Thus the following Higgs were introduced [17],

$$H_{1,2}^{(-1)}, \bar{H}_{1,2}^{(1)}, H_{1,2}^{(-2)}, \bar{H}_{1,2}^{(2)}, H_{1,2}^{(3)}, \bar{H}_{1,2}^{(-3)}, H_{1,2}^{(4)}, \bar{H}_{1,2}^{(-4)}, H_{1,2}^{(8)}, \bar{H}_{1,2}^{(-8)}, \tag{12}$$

where the $U(1)_X$ charges are given in parentheses, and $H_{1,2}^{(x)}$ have hypercharges $Y/2 = -1/2, 1/2$, and $\bar{H}_{1,2}^{(-x)}$ have hypercharges $Y/2 = 1/2, -1/2$, respectively. The idea is that the Higgs $H_{1,2}^{(x)}$ have direct couplings to the lighter families and mix with the MSSM Higgs $H_{1,2}$ via singlet θ fields. Thus the *renormalisable* Higgs terms (where we have neglected the Yukawa couplings) are :

$$\left(\begin{array}{ccc} Q_1 & Q_2 & Q_3 \end{array} \right) \left(\begin{array}{ccc} H_{1,2}^{(8)} & H_{1,2}^{(3)} & H_{1,2}^{(4)} \\ H_{1,2}^{(3)} & H_{1,2}^{(-2)} & H_{1,2}^{(-1)} \\ H_{1,2}^{(4)} & H_{1,2}^{(-1)} & H_{1,2} \end{array} \right) \left(\begin{array}{c} U_1^c \\ U_2^c \\ U_3^c \end{array} \right). \tag{13}$$

For example, the renormalisable 33 operator is depicted in Fig.1.

Such direct Higgs couplings, allowed by the $U(1)_X$ symmetry, combined with Higgs mixing via singlet field insertions, lead to the effective non-renormalisable operators in Eq.9. For example the spaghetti diagram responsible for the 32 quark mixing term is illustrated in Fig.2. It is clear that such diagrams generate all the operators in Eq.10. By drawing such diagrams it becomes clear that additional heavy vector Higgs are required beyond those in the direct coupling matrix in Eq.13. It is easy to see that all Higgs charges in integer steps between 8 and -2 are required if all elements of the mixing matrix are to be non-zero. For example Cabibbo mixing requires the additional Higgs with charges 2 and 1 (plus their conjugates) so that the Higgs of charge 3 can step down to the Higgs of zero charge via three θ field insertions as shown in Fig.3.

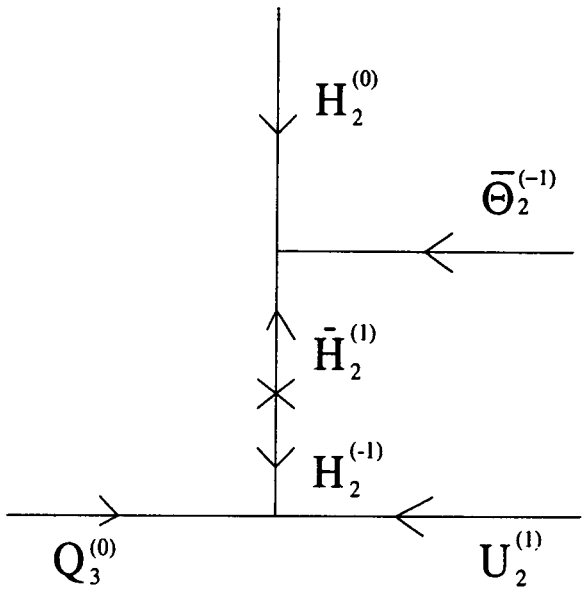

Figure 2: Spaghetti diagram for 32 mixing

The full list of Higgs required for this scenario is larger than assumed in Eq.12 and is displayed below:

$$H_{1,2}^{(8)}, \bar{H}_{1,2}^{(-8)}, H_{1,2}^{(7)}, \bar{H}_{1,2}^{(-7)}, H_{1,2}^{(6)}, \bar{H}_{1,2}^{(-6)}, H_{1,2}^{(5)}, \bar{H}_{1,2}^{(-5)}, H_{1,2}^{(4)}, \bar{H}_{1,2}^{(-4)},$$
$$H_{1,2}^{(3)}, \bar{H}_{1,2}^{(-3)}, H_{1,2}^{(2)}, \bar{H}_{1,2}^{(-2)}, H_{1,2}^{(1)}, \bar{H}_{1,2}^{(-1)}, H_{1,2}^{(-1)}, \bar{H}_{1,2}^{(1)}, H_{1,2}^{(-2)}, \bar{H}_{1,2}^{(2)} \quad (14)$$

Since complete Higgs mixing requires 20 Higgs vector representations, rather than 10 as assumed on the basis of the direct Higgs couplings, it is natural to try and look for a more economical alternative. This provides a motivation to study quark and lepton mixing in addition to Higgs mixing, as a means of generating the desired non-renormalisable operators. For example in Fig.4 we show a spaghetti diagram which can generate 32 mixing along the U^c line. Notice that we have added an intermediate quark $U^{(0)}$ with the same quantum numbers under the gauge symmetry of the model as U_3^c. In general, both will mix with $\bar{U}^{(0)}$ through a heavy mass term and we may always rotate the definition of the fields such that one of the linear combinations is massless. We identify this combination with the (conjugate) right handed top superfield of the MSSM and the other with the heavy field involved in the mass suppression of the spaghetti diagrams[3]. This means that vector quark and lepton states must be added, one chiral partner of which has the same X charge as a MSSM state. In Fig.5 we show how 32 mixing can be generated by mixing along the Q line.

[3]Wherever two fields with identical quantum numbers are present, one of which is a state of the MSSM, we will assume that this mixing has already been accounted for. The states labeled as MSSM states will thefore be defined as the massless linear combination.

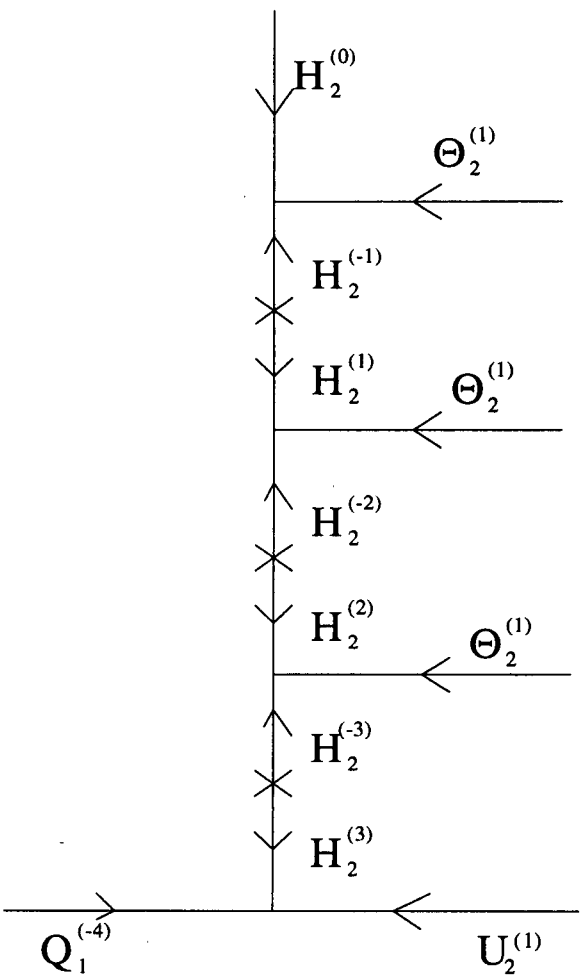

Figure 3: Spaghetti diagram for Cabibbo (12) mixing

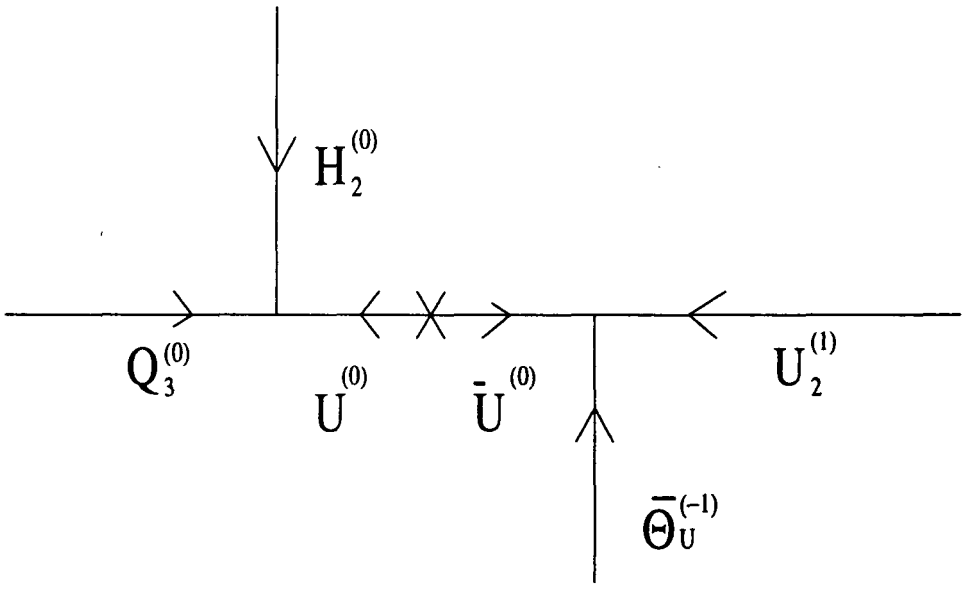

Figure 4: Spaghetti diagram for 32 mixing along the U line

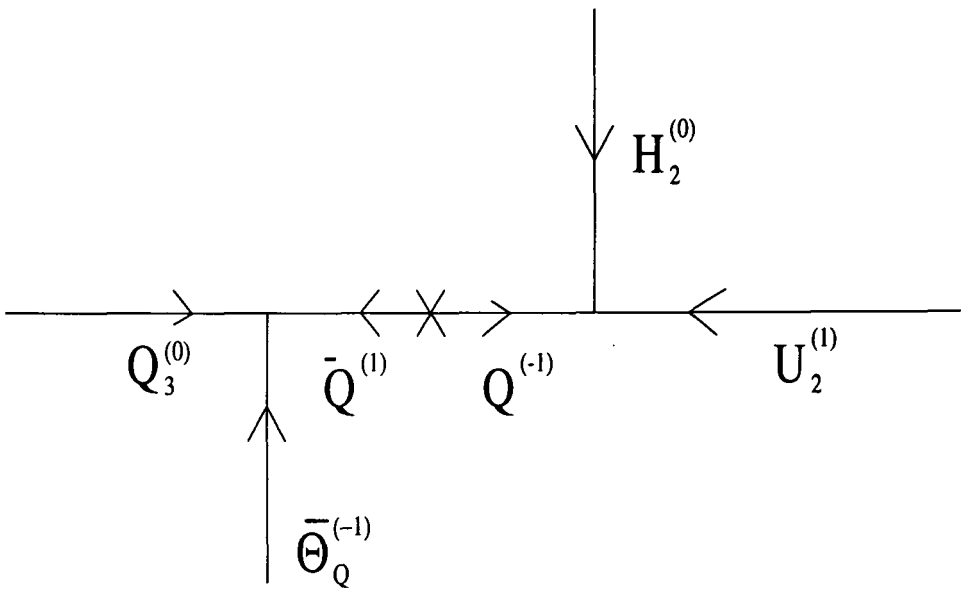

Figure 5: Spaghetti diagram for 32 mixing along the Q line

Similar diagrams can be drawn for the other mixings, and by consideration of such diagrams we can see that vector fields with X charges from -4 to 4 in integer steps are required. For example complete mixing along the Q line requires:

$$Q^{(-4)}, \bar{Q}^{(4)}, Q^{(-3)}, \bar{Q}^{(3)}, Q^{(-2)}, \bar{Q}^{(2)}, Q^{(-1)}, \bar{Q}^{(1)}, Q^{(0)}, \bar{Q}^{(0)}, \\ Q^{(1)}, \bar{Q}^{(-1)}, Q^{(2)}, \bar{Q}^{(-2)}, Q^{(3)}, \bar{Q}^{(-3)}, Q^{(4)}, \bar{Q}^{(-4)}. \tag{15}$$

corresponding to 9 vector $Q + \bar{Q}$ representations. Also, mixing along the U^c line requires 9 vector $U^c + \bar{U}^c$ representations; mixing along the D^c line requires 9 vector $D^c + \bar{D}^c$ representations; mixing along the L line requires 9 vector $L + \bar{L}$ representations; and mixing along the E^c line requires 9 vector $E^c + \bar{E}^c$ representations. In each case the X charges run from -4 to +4 in integer steps (plus the opposite charges for the conjugate states), as in Eq.15.

Now that we have allowed quark and lepton mixing (along the doublet and/or singlet lines) as well as Higgs mixing, many possibilities present themselves, corresponding to different combinations of each type of mixing. In the next section we shall use the constraint of string gauge unification to help to discriminate between the different possibilities. Here we shall make some general observations about the model building.

Let us begin with the U mass matrix. T We can envisage a scenario in which we have the 9 $Q + \bar{Q}$ fields listed in Eq.15, plus 9 vector $U^c + \bar{U}^c$ representations. In addition to these we also have the three chiral families with the X charges -4,1,0 as discussed above. To be more general we must also consider additional Higgs vector representations. We have seen that a possible Higgs mixing scenario requires 10 $H_2 + \bar{H}_2$ plus 10 $H_1 + \bar{H}_1$ extra Higgs with H charges from 8 to -2. However we may also wish to consider Higgs which couple any vector quark field to any other vector quark field, in which case the Higgs charges must range from 8 to -8. If for the moment we ignore the MSSM fields, but include all of the extra vector fields mentioned above then we have a 9×9 matrix of Higgs couplings to quark fields:

	$U^{(-4)}$	$U^{(-3)}$	$U^{(-2)}$	$U^{(-1)}$	$U^{(0)}$	$U^{(1)}$	$U^{(2)}$	$U^{(3)}$	$U^{(4)}$
$Q^{(-4)}$:	$H_2^{(8)}$	$H_2^{(7)}$	$H_2^{(6)}$	$H_2^{(5)}$	$H_2^{(4)}$	$H_2^{(3)}$	$H_2^{(2)}$	$H_2^{(1)}$	$H_2^{(0)}$
$Q^{(-3)}$:	$H_2^{(7)}$	$H_2^{(6)}$	$H_2^{(5)}$	$H_2^{(4)}$	$H_2^{(3)}$	$H_2^{(2)}$	$H_2^{(1)}$	$H_2^{(0)}$	$H_2^{(-1)}$
$Q^{(-2)}$:	$H_2^{(6)}$	$H_2^{(5)}$	$H_2^{(4)}$	$H_2^{(3)}$	$H_2^{(2)}$	$H_2^{(1)}$	$H_2^{(0)}$	$H_2^{(-1)}$	$H_2^{(-2)}$
$Q^{(-1)}$:	$H_2^{(5)}$	$H_2^{(4)}$	$H_2^{(3)}$	$H_2^{(2)}$	$H_2^{(1)}$	$H_2^{(0)}$	$H_2^{(-1)}$	$H_2^{(-2)}$	$H_2^{(-3)}$
$Q^{(0)}$:	$H_2^{(4)}$	$H_2^{(3)}$	$H_2^{(2)}$	$H_2^{(1)}$	$H_2^{(0)}$	$H_2^{(-1)}$	$H_2^{(-2)}$	$H_2^{(-3)}$	$H_2^{(-4)}$
$Q^{(1)}$:	$H_2^{(3)}$	$H_2^{(2)}$	$H_2^{(1)}$	$H_2^{(0)}$	$H_2^{(-1)}$	$H_2^{(-2)}$	$H_2^{(-3)}$	$H_2^{(-4)}$	$H_2^{(-5)}$
$Q^{(2)}$:	$H_2^{(2)}$	$H_2^{(1)}$	$H_2^{(0)}$	$H_2^{(-1)}$	$H_2^{(-2)}$	$H_2^{(-3)}$	$H_2^{(-4)}$	$H_2^{(-5)}$	$H_2^{(-6)}$
$Q^{(3)}$:	$H_2^{(1)}$	$H_2^{(0)}$	$H_2^{(-1)}$	$H_2^{(-2)}$	$H_2^{(-3)}$	$H_2^{(-4)}$	$H_2^{(-5)}$	$H_2^{(-6)}$	$H_2^{(-7)}$
$Q^{(4)}$:	$H_2^{(0)}$	$H_2^{(-1)}$	$H_2^{(-2)}$	$H_2^{(-3)}$	$H_2^{(-4)}$	$H_2^{(-5)}$	$H_2^{(-6)}$	$H_2^{(-7)}$	$H_2^{(-8)}$

(16)

There is of course a similar matrix of couplings involving the conjugate fields. Let us now introduce the three families of MSSM chiral fields shown below into the matrix in Eq.16:

$$Q_1^{(-4)}, Q_2^{(1)}, Q_3^{(0)}, U_1^{(-4)}, U_2^{(1)}, U_3^{(0)}, \tag{17}$$

where the family index is indicated by a subscript and the X charge is indicated by a superscript. The matrix now becomes a 12×12 matrix, and the Higgs content stays the same. We can now consider all possible ways in which mass mixing between the MSSM quarks can occur. In general for ij mixing we require a spaghetti diagram with the external lines consisting of Q_i, U_j, $H_2^{(0)}$. In addition we are allowed to hang any amount of θ and $\bar{\theta}$ spaghetti along any of the three lines Q, U, H_2 in order to achieve the mixing where the minimum amount of spaghetti corresponds to the leading non-renormalisable operator. To take a trivial example the 33 operator $Q_3 U_3 H_2^{(0)}$ is achieved directly at tree level without any spaghetti. At the other extreme the 11 operator $Q_1^{(-4)} U_1^{(-4)} H_2^{(0)}$ is clearly forbidden at tree level by the X symmetry, with the allowed non-renormalisable operator being $Q_1^{(-4)} U_1^{(-4)} H_2^{(0)} (\theta^{(1)})^8$. The required 8 pieces of θ spaghetti can be hung along any of the three lines Q, U, H_2 depending on the vector fields and charges which are assumed. For example in the Higgs mixing scenario of IR there is a tree level Higgs coupling $Q_1^{(-4)} U_1^{(-4)} H_2^{(8)}$ and the MSSM Higgs $H_2^{(0)}$ is achieved by stepping down the Higgs charge along the first row of the matrix in Eq.16 with the Higgs charge decreasing by one unit after each θ field insertion:

$$H_2^{(8)} \stackrel{\theta^{(1)}}{\to} H_2^{(7)} \stackrel{\theta^{(1)}}{\to} H_2^{(6)} \stackrel{\theta^{(1)}}{\to} H_2^{(5)} \stackrel{\theta^{(1)}}{\to} H_2^{(4)} \stackrel{\theta^{(1)}}{\to} H_2^{(3)} \stackrel{\theta^{(1)}}{\to} H_2^{(2)} \stackrel{\theta^{(1)}}{\to} H_2^{(1)} \stackrel{\theta^{(1)}}{\to} H_2^{(0)} \qquad (18)$$

with all the spaghetti mixing along the Higgs line. With the additional vector Q and U^c fields considered above there are alternative ways in which the spaghetti mixing can take place. For example we could begin from the non-renormalisable operator $Q_1^{(-4)} U^{(4)} H_2^{(0)}$ and step down the the U line to reach the desired $U_1^{(-4)}$ field:

$$U^{(4)} \stackrel{\bar{\theta}_U^{(1)}}{\to} U^{(3)} \stackrel{\bar{\theta}_U^{(1)}}{\to} U^{(2)} \stackrel{\bar{\theta}_U^{(1)}}{\to} U^{(1)} \stackrel{\bar{\theta}_U^{(1)}}{\to} U^{(0)} \stackrel{\bar{\theta}_U^{(1)}}{\to} U^{(-1)} \stackrel{\bar{\theta}_U^{(1)}}{\to} U^{(-2)} \stackrel{\bar{\theta}_U^{(1)}}{\to} U^{(-3)} \stackrel{\bar{\theta}_U^{(1)}}{\to} U_1^{(-4)} \qquad (19)$$

The resulting spaghetti diagram now has all the mixing along the U line, but is of the same order as the previous diagram. We could repeat this starting instead from the non-renormalisable operator $Q^{(4)} U_1^{(-4)} H_2^{(0)}$ and step down the the Q line to reach the desired $Q_1^{(-4)}$ field:

$$Q^{(4)} \stackrel{\bar{\theta}_Q^{(1)}}{\to} Q^{(3)} \stackrel{\bar{\theta}_Q^{(1)}}{\to} Q^{(2)} \stackrel{\bar{\theta}_Q^{(1)}}{\to} Q^{(1)} \stackrel{\bar{\theta}_Q^{(1)}}{\to} Q^{(0)} \stackrel{\bar{\theta}_Q^{(1)}}{\to} Q^{(-1)} \stackrel{\bar{\theta}_Q^{(1)}}{\to} Q^{(-2)} \stackrel{\bar{\theta}_Q^{(1)}}{\to} Q^{(-3)} \stackrel{\bar{\theta}_Q^{(1)}}{\to} Q_1^{(-4)} \qquad (20)$$

The resulting spaghetti diagram now has all the mixing along the Q line, but is of the same order as the previous diagram. There are of course many other possibilities which involve a combination of the three types of mixing, and all these possibilities will lead to non-renormalisable operators of the same order. For example suppose we again wish to generate the 11 operator $Q_1^{(-4)} U_1^{(-4)} H_2^{(0)} (\theta^{(1)})^8$ starting from the tree level operator $Q^{(-2)} U^{(-2)} H_2^{(4)}$. Now in order to achieve this we must have all three types of mixing simultaneously:

$$H_2^{(4)} \stackrel{\theta^{(1)}}{\to} H_2^{(3)} \stackrel{\theta^{(1)}}{\to} H_2^{(2)} \stackrel{\theta^{(1)}}{\to} H_2^{(1)} \stackrel{\theta^{(1)}}{\to} H_2^{(0)} \qquad (21)$$

$$U^{(-2)} \stackrel{\bar{\theta}_U^{(1)}}{\to} U^{(-3)} \stackrel{\bar{\theta}_U^{(1)}}{\to} U_1^{(-4)} \qquad (22)$$

$$Q^{(-2)} \overset{\bar{\theta}^{(1)}_{Q}}{\to} Q^{(-3)} \overset{\bar{\theta}^{(1)}_{Q}}{\to} Q_1^{(-4)} \tag{23}$$

Again the 11 operator is eighth order, but now there are four pieces of spaghetti from the Higgs line, two from the U line and two from the Q line. There are clearly many other possible ways of achieving 11 U mixing. The discussion of the other U mixings is similar. Finally the discussion of the D and E mixing matrices follows a similar pattern. The most general model clearly involves 9 vector copies of each of $(Q+\bar{Q}),(U+\bar{U}),(D+\bar{D}),(L+\bar{L}),(E+\bar{E})$, where we denote the number of vector copies as n_Q, n_U, n_D, n_L, n_E respectively, plus 16 vector copies of each of the Higgs fields $(H_2+\bar{H}_2),(H_1+\bar{H}_1)$, where we denote the number of vector copies as n_{H_1}, n_{H_2}, respectively.

This is clearly not the most economical model. For example the Ross[17] model is based on no extra vector quarks and leptons and 10 vector copies of each of $(H_2+\bar{H}_2),(H_1+\bar{H}_1)$. In the next section we shall impose the constraint of string gauge unification in order to try to determine a more economical model. However it is clear from the discussion of this section, that if too few extra vector states are allowed, then the required mass mixing will not be achievable. Therefore we seek the minimal model which is consistent with the constraints of spaghetti mixing discussed here, and string gauge unification. Since mixing can be achieved by a combination of mixing along the three different lines of the spaghetti diagram, in the next section we shall impose the following conservative lower limits on the minimal numbers of vector copies of fields. From U mixing we require:

$$n_Q + n_2 + n_U \geq 8. \tag{24}$$

From D mixing we require:

$$n_Q + n_2 + n_D \geq 8. \tag{25}$$

From E mixing we require:

$$n_2 + n_E \geq 8. \tag{26}$$

where for convenience we have defined the total number of doublets as

$$n_2 \equiv n_{H_1} + n_{H_2} + n_L. \tag{27}$$

In addition we shall allow for exotic superfields known as "sextons" S which are colour triplets, electroweak singlets and have hypercharge $1/6$. The sextons occur together with their vector conjugate $(S+\bar{S})$ and we denote the number of vector copies of sextons as n_S. These superfield representations are present in the massless spectrum of some string models [20].

3 String gauge unification analysis

We now describe the numerical constraints placed upon the models to ensure that they provide agreement with the low energy data, string scale gauge unification and

are compatible with models of fermion mass and mixing. Since we are hoping to eventually embed the model into a free-fermionic Kac-Moody level 1 string model, we must make sure that the gauge couplings obey the constraint of gauge unification at the string scale as in Eq.1. Another constraint comes from the agreement with the empirically determined values of the gauge couplings at low energy scales [21]. The data used is

$$\begin{aligned} \alpha(M_Z)^{-1} &= 127.90 \pm 0.09 \\ \sin^2\theta_w &= 0.2315 \pm 0.0002 \\ \alpha_S(M_Z) &= 0.118 \pm 0.003, \end{aligned} \tag{28}$$

where the numbers quoted are those derived in the $\overline{MS}$ renormalisation scheme from experiments. In what follows, we shall assume central values for $\alpha(M_Z)^{-1}, \sin^2\theta_W$ because their errors are comparatively small. The third constraint comes from the fact that we are expecting to use the intermediate matter as the heavy fields in a family $U(1)_X$ model of fermion masses. As previously demonstrated [18], these models require M_I to be within a couple of orders of magnitude of M_X to make the GSW anomaly cancellation mechanism work consistently. After some other filtering of models, as described below, the condition imposed on any successful model will be

$$M_I/M_X \geq 1/40. \tag{29}$$

Previous models of $U(1)_X$ family symmetry require a GUT type normalisation of Y from the anomaly cancellation conditions. Therefore, our condition upon the unification of gauge couplings will be

$$g_1(M_X) \equiv \sqrt{\frac{5}{3}}\frac{Y(M_X)}{2} = g_2(M_X) = g_3(M_X), \tag{30}$$

corresponding to a Kac-Moody level 1 string model with $k_1 = 5/3$. Finally, bearing in mind the long-term view of requiring the intermediate sector to mediate masses and mixings to all of the SM fermions, we impose Eqs.24-26 We then search through all of the models satisfying Eqs.24-26 for n_Q, n_2, n_U, n_D, $n_E \leq 10$ in order to find the models with less field content.

We now describe the systematic procedure to determine the models that pass the constraints[4] given by Eqs.24-26,28-30. Because of computer time constraints, we were not able to determine the predictions to two-loop order of every model satisfying Eqs.24-26. The following procedure was therefore adopted: the predictions for every different choice of intermediate field content were determined to one loop order as in [13] for $k_1 = 5/3$. If the one-loop predictions did not satisfy certain constraints to be described shortly, the models were discarded. For any models passing the previous "cut", the predictions were obtained at two-loop order.

The first one-loop filtering procedure was as follows: once a model has been selected by a a particular choice of intermediate matter, a guess ($M_X{}'$) of the string

[4]In fact, we will allow the prediction of $\alpha_S(M_Z)$ to be within 2σ of the value quoted in Eq.28.

unification scale was made. The condition $\alpha_1(M_X{}') = \alpha_2(M_X{}')$ yields a value of M_I consistent with unification at M_X by solving the one-loop RGEs for α_1 and α_2 in the $\overline{MS}$ scheme to obtain

$$\begin{aligned}\ln M_I &= \Big(2\pi(\alpha_2^{-1}(M_Z) - \alpha_1^{-1}(M_Z)) - \frac{77}{10}\ln M_Z + \frac{13}{30}\ln m_t + \frac{5}{3}\ln M_{SUSY} \\ &\quad -(3n_Q + n_2 - \frac{56}{10} - \frac{6}{10}Y_T)\ln M_X{}'\Big)/(Y_T\frac{3}{5} - 3n_Q - n_2), \end{aligned} \tag{31}$$

where $Y_T \equiv \sum_i (Y_i/2)^2$, i runs over all of the intermediate states and Y_i denotes the hypercharge of the intermediate state i. Throughout the numerical analysis, the entire SUSY spectrum was assumed to be at an effective scale equal to M_{SUSY}. Any threshold effects were taken into account by a step function approximation. With M_I and $M_X{}'$ values consistent with gauge unification at a scale $M_X{}'$, we could calculate M_X consistent with string scale unification in Eq.1 by finding

$$\begin{aligned}\alpha_2^{-1}(M_X) &= \alpha_2^{-1}(M_Z) + \frac{25}{12\pi}\ln\frac{m_t}{M_Z} + \frac{19}{12\pi}\ln\frac{M_{SUSY}}{m_t} - \frac{1}{2\pi}\ln\frac{M_I}{M_{SUSY}} \\ &\quad -\frac{1+3n_Q+n_2}{2\pi}\ln\frac{M_X}{M_I} \end{aligned} \tag{32}$$

and substituting it into Eq.1. To obtain values of M_X, M_I consistent both with $\alpha_1(M_X) = \alpha_2(M_X)$ and Eq.1, we now substitute $M_X{}'$ with M_X and iterate the above procedure until $M_X = M_X{}'$ is satisfied to some required accuracy. This yields a prediction for $\alpha_3(M_Z)$ by using $\alpha_3(M_X) \equiv \alpha_G$ where α_G is the string scale unified gauge structure constant. α_3 is then run to low energies using the one loop RGEs,

$$\begin{aligned}\alpha_3^{-1}(M_Z) &= \alpha_G(M_X) + \frac{23}{6\pi}\ln M_Z - \frac{1}{3\pi}\ln m_t - \frac{2}{\pi}\ln M_{SUSY} - \\ &\quad \frac{2n_Q + n_U + n_D}{2\pi}\ln M_I - \frac{3 - 2n_Q - n_U - n_D}{2\pi}\ln M_X. \end{aligned} \tag{33}$$

We have set $M_{SUSY} = m_t$, which[5] we take to be 166 GeV, corresponding to a top quark pole mass of 180 GeV for central values of $\alpha_S(M_Z)$, as in ref. [21]. We will return later to the effect of the empirical errors upon the inputs. We now require each model to pass the cuts $\alpha_S(M_Z) \leq 0.124$ and $M_I/M_X \geq 1/100$ to be worthy of the two-loop analysis. Note that these constraints are purposefully less severe than the ones in Eqs.28,29 because we do not want to discard models in which the imprecise one-loop predictions do not pass the more restrictive constraints, but in which the two-loop predictions pass.

Having attained a list of all models that passed the initial cuts, the two-loop predictions were then attained. At the two-loop level, the third family Yukawa couplings all effect the running of the gauge couplings and therefore the predictions of gauge unification. To a good approximation, the other Yukawa couplings of the MSSM have a negligible effect upon the running. As a starting point we must then obtain the values of these couplings at a particular scale, for a chosen value of $\tan\beta$ and $\alpha_S(M_Z)$.

[5] m_t denotes the running top mass in the $\overline{DR}$ renormalisation scheme.

Once we have selected these two parameters, we may determine the renormalised masses $m_{t,b,\tau}(m_t)$ of the top, bottom and tau particles at the renormalisation scale m_t, by running the three loop QCD $\otimes$ one loop QED RGEs through quark thresholds between m_τ and M_{SUSY} in the $\overline{MS}$ scheme [22]. $\alpha_S(\mu < M_Z)$ is actually run using a state of the art four loop QCD beta function [23]. In fact, the four loop contribution only changes the predictions by a few parts per thousand. This fact has a limited significance because the coefficient functions required to extract $\alpha_S(M_Z)$ from data are only known to at most two loops. The three gauge couplings are also run between M_Z and m_t in the $\overline{MS}$ scheme, assuming the particle spectrum of The Standard Model without the Higgs or top quark. The third-family $\overline{MS}$ Yukawa couplings may then be determined by [24]

$$\begin{aligned} \lambda_t(m_t) &= \frac{m_t(m_t)\sqrt{2}}{v \sin\beta} \\ \lambda_{b,\tau}(m_t) &= \frac{m_{b,\tau}(m_t)\sqrt{2}}{v \cos\beta}, \end{aligned} \tag{34}$$

where $v = 246.22$ GeV is the scale parameter of electroweak symmetry breaking. Above m_t, we wish to use the RGEs for the MSSM contained in Appendix 1. However these are in the $\overline{DR}$ scheme and so at m_t we match all of the quantities obtained in the $\overline{MS}$ scheme to the $\overline{DR}$ scheme. A guess for the intermediate scale M_I is chosen and the gauge couplings and third family Yukawa couplings are run to this scale. Above M_I, the effect of the intermediate matter is felt and the RGEs change as prescribed in Appendix 1. The couplings are run up in scale until either it becomes non-perturbative (which we take to be greater than 4) or until $g_1(\mu) = g_2(\mu)$. In the first case the value of M_I chosen is abandoned and in the second a prediction for $\alpha_3(m_t)$ is obtained by using the gauge unification condition. This is implemented by setting $g_3(\mu) = g_2(\mu)$ and then running all of the couplings down to m_t taking the intermediate matter into account and integrating it out of the effective theory at M_I. We may now iterate the above procedure using the previous predicted value of $g_3(m_t)$ as an input each time until $\alpha_3(m_t)$ converges and we have a value consistent with gauge unification with the intermediate matter at the guess value of M_I. The above procedure is then repeated for different values of M_I until a value is found in which the gauge couplings and unification scale satisfy Eq.1, i.e. the constraint of string scale gauge unification. It is a simple matter to re-convert $\alpha_3(m_t)$ back into the $\overline{MS}$ scheme and run back down to determine $\alpha_S(M_Z)$. Thus, for a given $\tan\beta$, we now have the predictions $M_I, \alpha_S(M_Z)$ that come from the assumption of string scale gauge unification. The conditions in Eqs.28,29 are then employed to remove any models which do not agree with the data or fit into the type of models of fermion masses being considered.

Tables 3,4 display the results of the algorithm described above for $\tan\beta = 43, 5$ respectively. The constraints we impose upon the models are so tight that out of the tens of thousand models examined, only a few models pass the constraints in each case. Note that for $\tan\beta = 43$, only two of these give $\alpha_S(M_Z)$ predictions within 1σ of the central value. The minimum number of extra vector multiplets added is

n_2	n_Q	n_U	n_D	n_E	$\alpha_3(M_Z)$	$M_X/10^{18}$ GeV	$M_I/10^{17}$ GeV
0	9	4	10	8	0.1173	0.5763	0.3387
0	10	5	10	8	0.1236	0.5457	0.5416
1	9	5	10	7	0.1172	0.5925	0.3428
1	10	6	10	7	0.1235	0.5565	0.5466
2	10	7	10	6	0.1234	0.5681	0.5520
3	10	8	10	5	0.1233	0.5808	0.5579
4	10	9	10	4	0.1232	0.5946	0.5644
5	10	10	10	3	0.1231	0.6098	0.5716

Table 3: Predictions of models that successfully unify the gauge couplings at M_X and provide enough intermediate matter to build a model of fermion masses for $\tan\beta = 43$.

n_2	n_Q	n_U	n_D	n_E	$\alpha_3(M_Z)$	$M_X/10^{18}$ GeV	$M_I/10^{17}$ GeV
0	9	4	10	8	0.1198	0.5700	0.3696
1	9	5	10	7	0.1196	0.5850	0.3737

Table 4: Predictions of models that successfully unify the gauge couplings at M_X and provide enough intermediate matter to build a model of fermion masses for $\tan\beta = 5$.

32. Varying $m_t^{phys}, \sin^2\theta_w$ between their 1σ limits can make a difference to $\alpha_S(M_Z)$ predictions of $\sim \pm 0.002$. The M_I/M_X prediction is hardly affected by the change in the input parameters. Varying $\alpha_1(M_Z)$ within its 1σ limits makes only a negligible change to the predictions. We note that the greatest uncertainty in our two-loop calculation is likely to be that due to threshold effects. Until now we have assumed that all of the intermediate matter lies at one scale M_I. While this is in some sense the simplest scheme, in general there could be some splittings between the different types of additional matter. One may naively expect these to not span more than one order of magnitude, but even given this constraint there could be significant errors due to the non-degeneracy. Non-degeneracy of the superpartner spectrum could also cause errors in the predictions. If we allow the presence of sexton fields, there are some additional possible models that the algorithm just described will not find. These are models with equal one-loop beta functions above M_I. In this case, the one-loop algorithm fails because the solution to $g_1(\mu) = g_2(\mu) = g_3(\mu)$ is not unique. Above M_I, the gauge couplings have slopes that differ by small two-loop effects. It is a simple matter to demonstrate that the models

$$\begin{aligned} n_Q &= 0,\ n_S = 24,\ n_2 - n_D = 20; \\ n_Q &= 1,\ n_S = 16,\ n_2 - n_D = 11; \\ n_Q &= 2,\ n_S = 8,\ n_2 - n_D = 2; \\ n_Q &= 3,\ n_S = 0,\ n_2 - n_D = 7; \end{aligned} \tag{35}$$

n_2	n_Q	n_U	n_D	n_E	n_S	$\alpha_3(M_Z)$	$M_X/10^{18}$ GeV	$M_I/10^{17}$ GeV
20	0	0	0	0	24	0.1218	0.4979	0.2906
21	0	0	1	0	24	0.1218	0.5069	0.2940
11	1	0	0	0	16	0.1226	0.4529	0.2788
12	1	0	1	0	16	0.1225	0.4593	0.2815

Table 5: Predictions of models that successfully unify the gauge couplings at M_X and provide enough intermediate matter to build a model of fermion masses for $\tan\beta = 43$. The models shown here belong to the special class of models that possess equal one-loop beta functions.

have the property of equal one-loop beta functions above M_I. Some of these models were investigated with an accurate version of the two-loop algorithm. Table 5 displays the predictions of a subset of the successful models in Eq.35.

4 Infra-Red Fixed Points

We now turn to the question of infra-red fixed points (IRFPs) of the dimensionless Yukawa couplings for the class of models which are consistent with the generation of acceptable textures via spaghetti mixing, and string gauge unification. Our discussion follows that of the IRFPs for the Ross model of Higgs mixing [17]. The basic idea behind this approach is the observation that, since there are no small dimensionless Yukawa couplings, it is possible that there are IRFP's analogous to the Pendleton-Ross fixed point [14]. Such fixed points are very welcome in this approach since the textures result from a large number of unknown Yukawa couplings, which would otherwise render this approach quite unpredictive. In addition the presence of a gauged family symmetry such as $U(1)_X$ is in principle quite dangerous since its presence can lead to large off-diagonal squark and slepton masses which can mediate flavour-changing processes at low energy. In particular the D term associated with $U(1)_X$ is in general only approximately flat due to lifting by soft supersymmetry breaking terms, and this can lead to family-dependent squark and slepton masses with unacceptably large mass splittings. This is a generic problem of any model with a gauged family symmetry, however the $U(1)_X$ symmetry here is non-asymptotically free with a large beta function so that its gauge coupling rapidly becomes very small below the string scale, leading to small X gaugino masses. It has been suggested [16] that the possible infra-red structure of the theory could help by relating the soft scalar masses to the small gaugino masses, thereby making them naturally smaller than the squark and slepton masses, or by enforcing $< \theta >=< \bar{\theta} >$ as an infra-red fixed point of the theory. We refer the reader to ref.[16] for more details. Here we shall only focus on the IRFPs of the dimensionless Yukawa couplings however.

4.1 The Top Quark Yukawa Coupling

The first step in finding the IRFPs of the theory is to construct the RGEs of the dimensionless Yukawa couplings of the theory. In supersymmetric theories this task is made quite simple, at least at the one loop level, by the observation that only the wavefunction diagrams contribute to the RGEs. The vertex contributions vanish due to the non-renormalisation theorem. This allows the RGEs to be constructed in a very straightforward manner. To take a simple example, consider a toy theory which only involves the top quark Yukawa coupling in the superpotential:

$$W = hQt^cH_2. \tag{36}$$

Defining the Yukawa and three gauge coupling parameters as

$$Y^h = \frac{h^2}{16\pi^2}, \ \tilde{\alpha}_i = \frac{g_i^2}{16\pi^2}, \tag{37}$$

and the scale variable as

$$t = -\ln(\mu^2) \tag{38}$$

we can write the RGE for the top quark Yukawa coupling as

$$\frac{dY^h}{dt} = Y^h(N_Q + N_{t^c} + N_{H_2}) \tag{39}$$

where N_i are the wavefunction renormalisation contributions from each of the three legs of the vertex. In the toy model the wavefunction diagrams are shown in Fig.6.

The wavefunction renormalisation contributions are explicitly,

$$\begin{aligned} N_Q &= \sum_i 2C_{2i}(Q)\tilde{\alpha}_i - Y^h \\ N_{t^c} &= \sum_i 2C_{2i}(t^c)\tilde{\alpha}_i - 2Y^h \\ N_{H_2} &= \sum_i 2C_{2i}(H_2)\tilde{\alpha}_i - 3Y^h \end{aligned} \tag{40}$$

where $2C_{2i}(R)$ is the quadratic Casimir of the representation R under the $i-th$ gauge group factor of the MSSM, arising from the gauge boson exchange corrections, and the multiplicity factors in front of the Y^h terms are due to doublet and colour counting for the particles going round the loop. Thus the RGE is explicitly

$$\frac{dY^h}{dt} = Y^h(\sum_{i,R} 2C_{2i}(R)\tilde{\alpha}_i - 6Y^h) \tag{41}$$

Now let us assume that in our toy model all three gauge couplings were equal, and all three gauge beta functions were equal (quite unrealistic for the low energy Yukawa coupling, but typical of the situation near the string scale). Then the RGE may be written as

$$\frac{dY^h}{dt} = Y^h(r\tilde{\alpha} - 6Y^h) \tag{42}$$

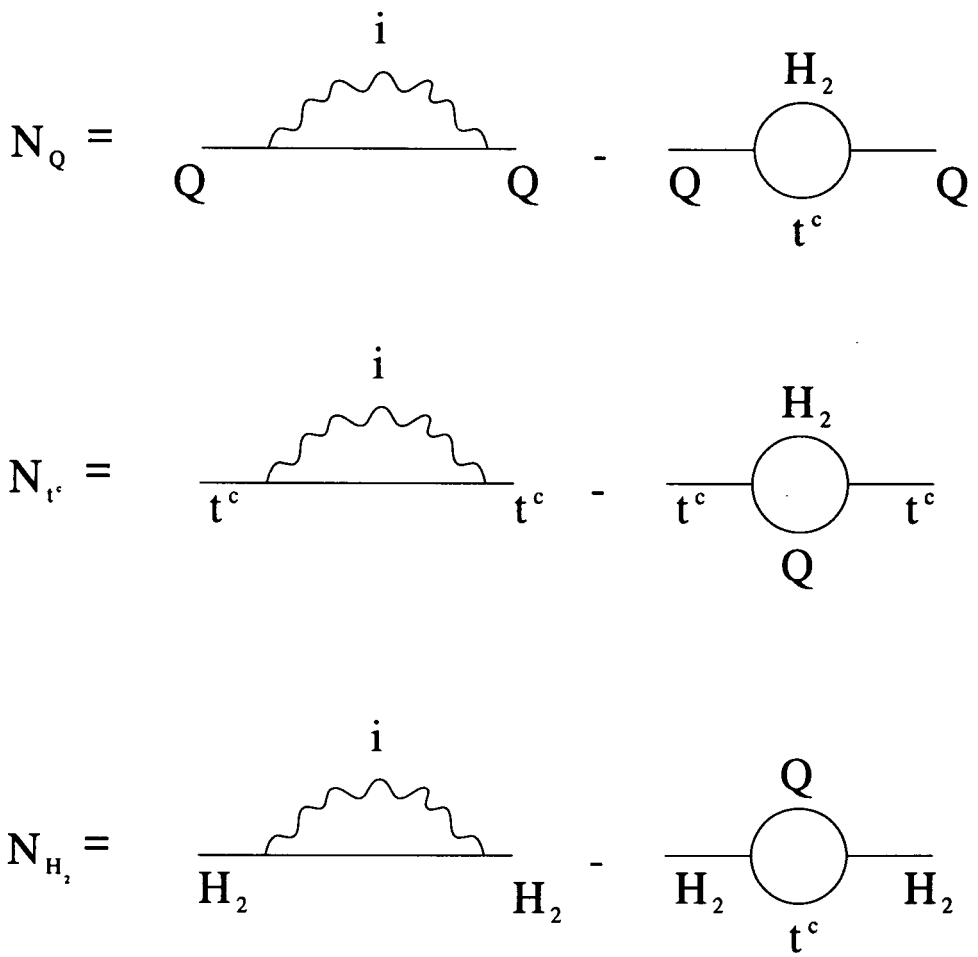

Figure 6: Contributions to the wavefunction renormalisation of the top quark Yukawa coupling.

where we have defined

$$r \equiv \sum_{i,R} 2C_{2i}(R) \tag{43}$$

where R runs over all fields involved in the coupling Y^h. We have written the three equal gauge couplings as $\tilde{\alpha}$. We now write the one loop gauge running as

$$\frac{\partial \tilde{\alpha}}{\partial t} = -b\tilde{\alpha}^2 \tag{44}$$

and define the ratio of Yukawa to gauge coupling as

$$R^h \equiv \frac{Y^h}{\tilde{\alpha}} \tag{45}$$

Then the RGE for this ratio is:

$$\frac{dR^h}{dt} = \tilde{\alpha}R^h(r + b - 6R^h) \tag{46}$$

and the Pendleton-Ross fixed point is given by $\frac{dR^h}{dt} = 0$. This condition can be achieved by

$$r + b - 6R^h = 0. \tag{47}$$

In terms of wavefunction renormalisation parameters, the RGE can be expressed as:

$$\frac{dR^h}{dt} = R^h(N_Q + N_{t^c} + N_{H_2} + \tilde{\alpha}b). \tag{48}$$

The fixed point condition can be expressed as[6]:

$$N_Q + N_{t^c} + N_{H_2} + \tilde{\alpha}b = 0. \tag{49}$$

4.2 The General Model

Ross [17] applied the above techniques to find the IRFPs of the Higgs mixing model. We wish to extend the discussion to the more general situation of n_Q, n_U, n_D, n_L, n_E copies of the vector representations

$$(Q^{(x)} + \bar{Q}^{(-x)}),\ (U^{c(y)} + \bar{U}^{c(-y)}),\ (D^{c(y)} + \bar{D}^{c(-y)}),\ (L^{(x)} + \bar{L}^{(-x)}),\ (E^{(y)} + \bar{E}^{c(-y)}) \tag{50}$$

plus n_{H_1}, n_{H_2} copies of the vector representations

$$(H_2^{(z)} + \bar{H}_2^{(-z)}),\ (H_1^{(z)} + \bar{H}_1^{(-z)}) \tag{51}$$

[6]It is worth noting that an alternative fixed point has recently been proposed by Jack and Jones [25], in which $\frac{dR^h}{dt} = 0$ is achieved by the more stringent conditions:$N_Q = N_{t^c} = N_{H_2} = -\frac{1}{3}\tilde{\alpha}b$. These conditions may be expressed in a more general way, and are valid to two loops. However they are not satisfied for our simple toy model, and they will not be of use for our more general model.

where we have labeled the vector fields by their X charges x, y, z. For the special case of $z = 0$ the Higgs are identified with the two MSSM Higgs doublets,

$$H_1^{(0)},\ H_2^{(0)} \tag{52}$$

and do not have vector conjugates. The above fields are in addition to the three chiral families of quarks and leptons which we label as:

$$Q_i,\ U_j^c,\ D_j^c,\ L_i,\ E_j^c \tag{53}$$

where we label these fields by the family index subscript $i, j = 1, \cdots 3$, but do not label their X charges (for $i, j = 1, 2, 3$ the X charges are -4,1,0, respectively, as discussed earlier). We introduce the X charge breaking singlet Higgs fields $(\theta_Q + \bar{\theta}_Q), (\theta_U + \bar{\theta}_U), (\theta_D + \bar{\theta}_D), (\theta_L + \bar{\theta}_L), (\theta_E + \bar{\theta}_E)$ plus $(\theta_2 + \bar{\theta}_2), (\theta_1 + \bar{\theta}_1)$ which change the X charge of the particular field by 1 or -1. We also introduce MSSM singlet Higgs with $X = 0$: $\Phi_Q, \Phi_U, \Phi_D, \Phi_L, \Phi_E$ plus Φ_2, Φ_1 whose VEVs are responsible for the heavy vector masses at a common scale M_I.

The most general model is then defined by the gauge group,

$$SU(3)_C \times SU(2)_L \times U(1)_Y \times U(1)_X \tag{54}$$

with the superpotential involving the chiral quarks and leptons containing the trilinear terms

$$\begin{aligned}
W_1 \;=\; & \sum_{i,j} h_{ij} Q_i U_j^c H_2^{(z)} + \sum_{i,j} k_{ij} Q_i D_j^c H_1^{(z)} + \sum_{i,j} l_{ij} L_i E_j^c H_1^{(z)} \\
+ \; & \sum_{i,y} h_{i(y)} Q_i U^{c(y)} H_2^{(z)} + \sum_{i,y} k_{i(y)} Q_i D^{c(y)} H_1^{(z)} + \sum_{i,y} l_{i(y)} L_i E^{c(y)} H_1^{(z)} \\
+ \; & \sum_{x,j} h_{(x)j} Q^{(x)} U_j^c H_2^{(z)} + \sum_{x,j} k_{(x)j} Q^{(x)} D_j^c H_1^{(z)} + \sum_{x,j} l_{(x)j} L^{(x)} E_j^c H_1^{(z)} \\
+ \; & \sum_i s_{Q_i} \theta_Q Q_i \bar{Q}^{(-x-1)} + \sum_j s_{U_j} \theta_U U_j^c \bar{U}^{c(-y-1)} + \sum_j s_{D_j} \theta_D D_j^c \bar{D}^{c(-y-1)} \\
+ \; & \sum_i s_{L_i} \theta_L L_i \bar{L}^{(-x-1)} + \sum_j s_{E_j} \theta_E E_j^c \bar{E}^{c(-y-1)} \\
+ \; & \sum_i \bar{s}_{Q_i} \bar{\theta}_Q Q_i \bar{Q}^{(-x+1)} + \sum_j \bar{s}_{U_j} \bar{\theta}_U U_j^c \bar{U}^{c(-y+1)} + \sum_j \bar{s}_{D_j} \bar{\theta}_D D_j^c \bar{D}^{c(-y+1)} \\
+ \; & \sum_i \bar{s}_{L_i} \bar{\theta}_L L_i \bar{L}^{(-x+1)} + \sum_j \bar{s}_{E_j} \bar{\theta}_E E_j^c \bar{E}^{c(-y+1)}.
\end{aligned} \tag{55}$$

In Eqs.55-56, it is to be understood that the X charges of the fields in each coupling must add to zero and that this decides the superscripts that are not summed over. This is true for all superpotentials and wave-function renormalisations listed in this paper. We neglect some terms in the superpotential that are not banned by the symmetries we have listed so far. Some of these are undesirable in terms of reproducing the correct phenomenology, and so we appeal to the extra U(1) symmetries that tend

to come with string-derived models to ban these terms. The remaining terms in the superpotential involving the extra vector states and Higgs are:

$$
\begin{aligned}
W_2 \;=\; & \sum_{x,y} h_{(xy)} Q^{(x)} U^{c(y)} H_2^{(z)} + \sum_{x,y} k_{(xy)} Q^{(x)} D^{c(y)} H_1^{(z)} \\
+ \; & \sum_{x,y} l_{(xy)} L^{(x)} E^{c(y)} H_1^{(z)} + \sum_{x,y} \bar{h}_{(x)(y)} \bar{Q}^{(-x)} \bar{U}^{c(-y)} \bar{H}_2^{(-z)} \\
+ \; & \sum_{x,y} \bar{k}_{(x)(y)} \bar{Q}^{(-x)} \bar{D}^{c(-y)} \bar{H}_1^{(-z)} + \sum_{x,y} \bar{l}_{(x)(y)} \bar{L}^{(-x)} \bar{E}^{c(-y)} \bar{H}_1^{(-z)} \\
+ \; & \sum_{z} r_{H_1^{(z)}} \Phi_{H_1} H_1^{(z)} \bar{H}_1^{(-z)} + \sum_{z} r_{H_2^{(z)}} \Phi_{H_2} H_2^{(z)} \bar{H}_2^{(-z)} \\
+ \; & \sum_{x} r_{Q^{(x)}} \Phi_Q Q^{(x)} \bar{Q}^{(-x)} + \sum_{y} r_{U^{(y)}} \Phi_U U^{c(y)} \bar{U}^{c(-y)} + \sum_{y} r_{D^{(y)}} \Phi_D D^{c(y)} \bar{D}^{c(-y)} \\
+ \; & \sum_{x} r_{L^{(x)}} \Phi_L L^{(x)} \bar{L}^{(-x)} + \sum_{y} r_{E^{(y)}} \Phi_E E^{c(y)} \bar{E}^{c(-y)} \\
+ \; & \sum_{z} s_{H_1^{(z)}} \theta_{H_1} H_1^{(z)} \bar{H}_1^{(-z-1)} + \sum_{z} \bar{s}_{H_1^{(z)}} \bar{\theta}_{H_1} H_1^{(z)} \bar{H}_1^{(-z+1)} \\
+ \; & \sum_{z} s_{H_2^{(z)}} \theta_{H_2} H_2^{(z)} \bar{H}_2^{(-z-1)} + \sum_{z} \bar{s}_{H_2^{(z)}} \bar{\theta}_{H_2} H_2^{(z)} \bar{H}_2^{(-z+1)} \\
+ \; & \sum_{x} s_{Q^{(x)}} \theta_Q Q^{(x)} \bar{Q}^{(-x-1)} + \sum_{x} \bar{s}_{Q^{(x)}} \bar{\theta}_Q Q^{(x)} \bar{Q}^{(-x+1)} \\
+ \; & \sum_{y} s_{U^{(y)}} \theta_U U^{c(y)} \bar{U}^{c(-y-1)} + \sum_{y} \bar{s}_{U^{(y)}} \bar{\theta}_U U^{c(y)} \bar{U}^{c(-y+1)} \\
+ \; & \sum_{y} s_{D^{(y)}} \theta_D D^{c(y)} \bar{D}^{c(-y-1)} + \sum_{y} \bar{s}_{D^{(y)}} \bar{\theta}_D D^{c(y)} \bar{D}^{c(-y+1)} \\
+ \; & \sum_{x} s_{L^{(x)}} \theta_L L^{(x)} \bar{L}^{(-x-1)} + \sum_{x} \bar{s}_{L^{(x)}} \bar{\theta}_L L^{(x)} \bar{L}^{(-x+1)} \\
+ \; & \sum_{y} s_{E^{(y)}} \theta_E E^{c(y)} \bar{E}^{c(-y-1)} + \sum_{y} \bar{s}_{E^{(y)}} \bar{\theta}_E E^{c(y)} \bar{E}^{c(-y+1)}
\end{aligned}
\tag{56}
$$

where in the first two lines of Eq.56, X symmetry requires that $z = -(x+y)$. Since the fields above are being labeled by their X charges, the limits of each of the summations will depend on the particular model under consideration. The family indices range from $i, j = 1, \cdots 3$. However in specific models only a subset of the fields will be present, and consequently not all of the terms will be present. For the moment we prefer to keep the values of n_Q, n_U, n_D, n_L, n_E and n_{H_1}, n_{H_2} general, however. Also, we have not written the most general superpotential allowed under the gauge symmetry since θ_E could couple to the vector quarks, for example. It is possible that $\theta_{Q,U,D,L,E,1,2}$ are identified with just one superfield and that ϕ_{Q,U,D,L,E,H_1,H_2} are also identified with one superfield (and similarly for the conjugate singlets).

The one-loop RGEs for the couplings R^h_{ij},R^k_{ij},R^l_{ij} are

$$
\begin{aligned}
\frac{dR^h_{ij}}{dt} &= R^h_{ij}(N_{Q_i} + N_{U^c_j} + N_{H_2^{(z)}} + \tilde{\alpha} b) \\
\frac{dR^k_{ij}}{dt} &= R^k_{ij}(N_{Q_i} + N_{D^c_j} + N_{H_1^{(z)}} + \tilde{\alpha} b)
\end{aligned}
$$

$$\frac{dR^l_{ij}}{dt} = R^l_{ij}(N_{L_i} + N_{E^c_j} + N_{H_1^{(z)}} + \tilde{\alpha}b) \tag{57}$$

where we have assumed the gauge couplings are approximately equal so that

$$\tilde{\alpha} \equiv \frac{5}{3}\tilde{\alpha}_1 = \tilde{\alpha}_2 = \tilde{\alpha}_3. \tag{58}$$

The full list of wavefunction renormalisations are given in appendix 2. The fixed point conditions for the chiral quark and lepton couplings, R^h_{ij},R^k_{ij},R^l_{ij}, are listed below:

$$\begin{aligned} N_{Q_i} + N_{U^c_j} + N_{H_2^{(z)}} + \tilde{\alpha}b &= 0 \\ N_{Q_i} + N_{D^c_j} + N_{H_1^{(z)}} + \tilde{\alpha}b &= 0 \\ N_{L_i} + N_{E^c_j} + N_{H_1^{(z)}} + \tilde{\alpha}b &= 0 \end{aligned} \tag{59}$$

We also require a similar fixed point for the couplings $R^h_{i(y)}$, $R^k_{i(y)}$, $R^l_{i(y)}$, and $R^h_{(x)j}$, $R^k_{(x)j}$, $R^l_{(x)j}$, that involve a mixture of chiral and vector fields. Also we require a fixed point for the couplings $R^h_{(xy)}$, $R^k_{(xy)}$, $R^l_{(xy)}$, involving purely vector fields. Similar fixed point conditions apply to the conjugate vector couplings, as well as all the singlet couplings. So every trilinear coupling will have a fixed point condition which is expressed in terms of the wavefunction renormalisations, similar to the above conditions. A fixed point is achieved when all the conditions are simultaneously satisfied. Note this assumes that none of the $R^{h,k,l}_{ij}$ couplings are zero at the fixed point, another set of possibilities allowed by Eq.57. We will not consider this here since many of the preceding arguments relied on the dimensionless couplings being $\sim O(1)$, rather than approximately zero. We merely note that in general there are 2^n fixed points in this multi-dimensional system of n couplings, all but one of which involve some of the dimensionless couplings being zero.

4.3 Conditions for Infra-Red Attractiveness

We now write the RG equations as

$$\frac{dR_i(t)}{dt} = \tilde{\alpha}R_i(t)\left[(r_i + b) - \sum_j S_{ij}R_j(t)\right], \tag{60}$$

where R_i now denotes the ratio of any Yukawa coupling i to the gauge coupling (squared), as prescribed by Eq.45. We have written $r_i \equiv 2\sum C_2(R_x)$, where the sum runs over simple gauge groups and the representations R_x under those gauge groups, x corresponding to the field that labels N_x of R_i in Eq.57. The fixed point condition is then satisfied when the right hand side of Eq.60 is zero for all i. First, we assume that none of the R_i is equal to zero at the fixed point, in which case

$$\sum_j S_{ij}R^*_j = r_i + b, \tag{61}$$

where we have denoted the value of R_j at the fixed point as R_j^*. The problem of locating the fixed points becomes a straightforward problem in linear algebra, albeit involving a large number of dimensions, corresponding to the large number of trilinear Yukawa couplings. The fixed points are given in principle by inverting the matrix S_{ij},

$$R_i^* = \sum_j (S^{-1})_{ij}(r_j + b) \tag{62}$$

To determine the infra-red stability of the system in Eq.60, we need to Taylor expand it around the fixed point given in Eq.61. We can then drop all except the linear terms, the resulting system of which allows an algebraic solution and can thus be tested for infra-red stability. We therefore make a change of variables to $\rho_i(t) \equiv R_i(t) - R_i^*$. The RGE Eq.60 then becomes

$$\frac{d\rho_i(t)}{dt} = -\tilde{\alpha}(t)(\rho_i(t) + R_i^*)\left[(r_i + b) - \sum_j S_{ij}(\rho_j(t) + R_j^*)\right], \tag{63}$$

where we have substituted the fixed point values of R_i^* from Eq.61. When we drop the quadratic term in Eq.63 and change the independent variable from t to $\tilde{\alpha}$ by Eq.44, we obtain the linearised system

$$\frac{d\rho_i(t)}{d\ln\tilde{\alpha}(t)} = \frac{1}{b}R_i^* \sum_j S_{ij}\rho_j(t). \tag{64}$$

Eq.64 then describes the behaviour of the trajectories as they approach the fixed point. It has solutions

$$\rho_i(t) = x_j\left(\tilde{\alpha}(t)\right)^{\lambda_j}, \tag{65}$$

where x_j, λ_j satisfy the eigenvalue equation

$$\begin{aligned} \sum_j A_{ij}x_j &= \lambda_i x_i \\ A_{ij} &\equiv \frac{1}{b}R_i^* S_{ij}. \end{aligned} \tag{66}$$

Because the expanded RGE Eq.64 is linear, the general solution is a linear combination of each ρ_i in Eq.64. Because R_j^*/b is a factor multiplying each row of the matrix S in Eq.66, we may factorise the eigenvalues as

$$\lambda_i \equiv \overline{\lambda}_i \prod_j R_j^*/b, \tag{67}$$

where $\overline{\lambda}_i$ are now just eigenvalues of S.

For $b > 0$ as in these models, $\tilde{\alpha}$ decreases with decreasing renormalisation scale μ. For the fixed point to be infra-red stable, we require every eigenvalue λ_i to have a positive real part, since then $\rho_i \to 0$ as μ decreases. $\lambda_i = 0$ corresponds to a direction in coupling space which is neither attracted nor repelled by the fixed point. For each of these directions there should be one free parameter in the solution to

the fixed point equations which embodies the information on where a solution lies along this direction (and is set by the initial boundary conditions). In the class of models presented here, this corresponds to some information about the string scale being retained at lower energies. Because $R_j^*, b > 0$ in Eq.67, this simply translates to the condition that every eigenvalue $\overline{\lambda}_i$ of S must possess a positive real part. Complex eigenvalues always come in complex conjugate pairs, as do their associated eigenvectors. Writing $\lambda_j \equiv k_j + is_j$, where k_j, s_j are real, the solution in this case is

$$x_j\tilde{\alpha}^{k_j+is_j} + x_j^*\tilde{\alpha}^{k_j-is_j} = \tilde{\alpha}^{k_j}\left[x_j\tilde{\alpha}^{is_j} + x_j^*\tilde{\alpha}^{-is_j}\right]. \tag{68}$$

Eq.68 describes a spiral-like trajectory, the distance to the fixed point being controlled by $\tilde{\alpha}^{k_j}$. Thus k_j must be positive for the trajectory to be infra-red stable. If these conditions are not met, the fixed point is either a saddle point or an ultra-violet fixed point and so the fixed point will never be achieved at low energies. We will see in the following specific models, examples of infra-red stable and saddle point behaviour. We will also see that the zero eigenvalue directions occur from a degeneracy in the fixed point equations.

4.4 Example 1: Higgs Mixing Model

As a first example of the general results, we calculate the fixed point solutions and the infra-red stability in a Higgs mixing model similar to that proposed by Ross [17]. In this model there are $n_{H_1} = 10, n_{H_2} = 10$ copies of the vector representations

$$(H_2^{(z)} + \bar{H}_2^{(-z)}),\ (H_1^{(z)} + \bar{H}_1^{(-z)}), \tag{69}$$

in the model, which means $n_2 = 20$. Ross also included some colour triplets which served the purpose of increasing the gauge unification scale although not enough to be consistent alone with string-scale gauge unification. We saw in Eq.35 that such a model has string scale gauge unification if $n_S = 24$, but we shall ignore the exotic sexton representations in the following analysis. The superpotential of the model is then

$$\begin{aligned} W &= \sum_{i,j} h_{ij}Q_iU_j^cH_2^{(z)} + \sum_{i,j} k_{ij}Q_iD_j^cH_1^{(z)} + \sum_{i,j} l_{ij}L_iE_j^cH_1^{(z)} \\ &+ \sum_{z=-2}^{8} r_{H_1^{(z)}}\Phi_{H_1}H_1^{(z)}\bar{H}_1^{(-z)} + \sum_{z=-2}^{8} r_{H_2^{(z)}}\Phi_{H_2}H_2^{(z)}\bar{H}_2^{(-z)} \\ &+ \sum_{z=-2}^{7} s_{H_1^{(z)}}\theta_{H_1}H_1^{(z)}\bar{H}_1^{(-z-1)} + \sum_{z=-1}^{8} \bar{s}_{H_1^{(z)}}\bar{\theta}_{H_1}H_1^{(z)}\bar{H}_1^{(-z+1)} \\ &+ \sum_{z=-2}^{7} s_{H_2^{(z)}}\theta_{H_2}H_2^{(z)}\bar{H}_2^{(-z-1)} + \sum_{z=-1}^{8} \bar{s}_{H_2^{(z)}}\bar{\theta}_{H_2}H_2^{(z)}\bar{H}_2^{(-z+1)}. \end{aligned} \tag{70}$$

It is to be understood in the first three terms Eq.70 that

$$z = -\text{Xcharge}(i^{th}\text{ family}) - \text{Xcharge}(j^{th}\text{ family}). \tag{71}$$

Therefore the Higgs which occur in the interactions with couplings $(h,k,l)_{ij}$ have charges as given below:

$$\begin{pmatrix} (h,k,l)_{11}H^{(8)}_{1,2} & (h,k,l)_{12}H^{(3)}_{1,2} & (h,k,l)_{13}H^{(4)}_{1,2} \\ (h,k,l)_{21}H^{(3)}_{1,2} & (h,k,l)_{22}H^{(-2)}_{1,2} & (h,k,l)_{23}H^{(-1)}_{1,2} \\ (h,k,l)_{31}H^{(4)}_{1,2} & (h,k,l)_{32}H^{(-1)}_{1,2} & (h,k,l)_{33}H_{1,2} \end{pmatrix} \tag{72}$$

The above Higgs having direct couplings are only a subset of the full list of required Higgses:

$$\begin{aligned} &H^{(8)}_{1,2}, \bar{H}^{(-8)}_{1,2}, H^{(7)}_{1,2}, \bar{H}^{(-7)}_{1,2}, H^{(6)}_{1,2}, \bar{H}^{(-6)}_{1,2}, H^{(5)}_{1,2}, \bar{H}^{(-5)}_{1,2}, H^{(4)}_{1,2}, \bar{H}^{(-4)}_{1,2}, \\ &H^{(3)}_{1,2}, \bar{H}^{(-3)}_{1,2}, H^{(2)}_{1,2}, \bar{H}^{(-2)}_{1,2}, H^{(1)}_{1,2}, \bar{H}^{(-1)}_{1,2}, H^{(-1)}_{1,2}, \bar{H}^{(1)}_{1,2}, H^{(-2)}_{1,2}, \bar{H}^{(2)}_{1,2} \end{aligned} \tag{73}$$

The one-loop wavefunction renormalisations from Appendix 2 are:

$$\begin{aligned} N_{Q_i} &= \frac{8}{3}\tilde{\alpha}_3 + \frac{3}{2}\tilde{\alpha}_2 + \frac{1}{18}\tilde{\alpha}_1 - \sum_j Y^h_{ij} - \sum_j Y^k_{ij} \\ N_{U^c_j} &= \frac{8}{3}\tilde{\alpha}_3 + \frac{8}{9}\tilde{\alpha}_1 - 2\sum_i Y^h_{ij} \\ N_{D^c_j} &= \frac{8}{3}\tilde{\alpha}_3 + \frac{2}{9}\tilde{\alpha}_1 - 2\sum_i Y^k_{ij} \\ N_{L_i} &= \frac{3}{2}\tilde{\alpha}_2 + \frac{1}{2}\tilde{\alpha}_1 - \sum_j Y^l_{ij} \\ N_{E^c_j} &= 2\tilde{\alpha}_1 - 2\sum_i Y^l_{ij} \end{aligned} \tag{74}$$

The Higgs wavefunction contributions are:

$$\begin{aligned} N_{H^{(z)}_1} &= \frac{3}{2}\tilde{\alpha}_2 + \frac{1}{2}\tilde{\alpha}_1 - 3\sum_{ij} Y^k_{ij} - \sum_{ij} Y^l_{ij} \\ &\quad - Y^{r}{}_{H^{(z)}_1} - Y^{s}{}_{H^{(z)}_1} - Y^{\bar{s}}{}_{H^{(z)}_1} \\ N_{H^{(z)}_2} &= \frac{3}{2}\tilde{\alpha}_2 + \frac{1}{2}\tilde{\alpha}_1 \\ &\quad - 3\sum_{ij} Y^h_{ij} - Y^{r}{}_{H^{(z)}_2} - Y^{s}{}_{H^{(z)}_2} - Y^{\bar{s}}{}_{H^{(z)}_2} \\ N_{\bar{H}^{(-z)}_1} &= \frac{3}{2}\tilde{\alpha}_2 + \frac{1}{2}\tilde{\alpha}_1 - Y^{r}{}_{H^{(z)}_1} - Y^{\bar{s}}{}_{H^{(z+1)}_1} - Y^{s}{}_{H^{(z-1)}_1} \\ N_{\bar{H}^{(-z)}_2} &= \frac{3}{2}\tilde{\alpha}_2 + \frac{1}{2}\tilde{\alpha}_1 - Y^{r}{}_{H^{(z)}_2} - Y^{\bar{s}}{}_{H^{(z+1)}_2} - Y^{s}{}_{H^{(z-1)}_2} \end{aligned} \tag{75}$$

The wavefunction contributions for the singlets are:

$$\begin{aligned} N_{\Phi_{H_1}} &= -2\sum_z Y^{r}{}_{H^z_1}, \; N_{\Phi_{H_2}} = -2\sum_z Y^{r}{}_{H^z_2} \\ N_{\theta_{H_1}} &= -2\sum_z Y^{s}{}_{H^z_1}, \; N_{\theta_{H_2}} = -2\sum_z Y^{s}{}_{H^z_2} \\ N_{\bar{\theta}_{H_1}} &= -2\sum_z Y^{\bar{s}}{}_{H^z_1}, \; N_{\bar{\theta}_{H_2}} = -2\sum_z Y^{\bar{s}}{}_{H^z_2}. \end{aligned} \tag{76}$$

Following Ross, we assume a general symmetric form for the matrices l, k, h at the string scale and use the fact that the RGEs Eq.60 respect this form. The solutions of the fixed point equations Eq.62 applied to this model are [17]

$$
\begin{aligned}
R^{h_{ij}} &= \left(\frac{887}{1728}+\frac{3\,b}{64}\right)\begin{pmatrix} 2 & 1 & 1 \\ 1 & 2 & 1 \\ 1 & 1 & 2 \end{pmatrix} \\
R^{k_{ij}} &= \begin{pmatrix} \frac{1297}{864}+\frac{5\,b}{32}-x-y & y & x \\ y & \frac{1297}{864}+\frac{5\,b}{32}-y-z & z \\ x & z & \frac{1297}{864}+\frac{5\,b}{32}-z-x \end{pmatrix} \\
R^{l_{ij}} &= \begin{pmatrix} -\frac{103}{72}-\frac{b}{8}+3x+3y & \frac{295}{192}+\frac{11\,b}{64}-3y & \frac{295}{192}+\frac{11\,b}{64}-3x \\ \frac{295}{192}+\frac{11\,b}{64}-3y & -\frac{103}{72}-\frac{b}{8}+3y+3z & \frac{295}{192}+\frac{11\,b}{64}-3z \\ \frac{295}{192}+\frac{11\,b}{64}-3x & \frac{295}{192}+\frac{11\,b}{64}-3z & -\frac{103}{72}-\frac{b}{8}+3x+3z \end{pmatrix}
\end{aligned} \tag{77}
$$

Eq.77 shows that there are 3 undetermined parameters at the fixed point. When we check the solution for infra-red stability we find that the eigenvalues of S are

$$
\begin{aligned}
\bar{\lambda}_i &= \{17.9, 12.8, 11.6, 9.57, 8.56, 11.1, 7.39, 4.16, 3.78, 5.06, 5.65, 3.81, 4.98, 6.0, \\
&\quad 4.66, 0, 0, 0\}.
\end{aligned} \tag{78}
$$

Eq.78 shows that the fixed point solution identified is completely infra-red stable, with three undetermined free parameters.

So far, in the limit that singlets are ignored, our results are in agreement with those of ref.[17]. Although the stability question was not addressed [17] we find that the fixed point is stable in the infra-red limit so all is well. Now we must consider the effect of the singlets. In the Ross model [17] the result was quoted that the singlet couplings of the Higgs Mixing Model are approximately flavour independent. We find that this is only valid if the extra Higgs doublets which do not have direct couplings to fermions are ignored. To be explicit, Ross considered a model with the only extra Higgs states being

$$
H^{(8)}_{1,2}, \bar{H}^{(-8)}_{1,2}, H^{(4)}_{1,2}, \bar{H}^{(-4)}_{1,2}, H^{(3)}_{1,2}, \bar{H}^{(-3)}_{1,2}, H^{(2)}_{1,2}, \bar{H}^{(-2)}_{1,2}, H^{(1)}_{1,2}, \bar{H}^{(-1)}_{1,2}. \tag{79}
$$

However we saw earlier that the full list of Higgs states in Eq.73 is required for correct Cabbibo mixing and CKM mixing. The full Higgs mixing model is analysed in Appendix 3 where we solve the 80 simultaneous equations for 80 unknowns (keeping the matrices k, l, h symmetric) to determine the stability and predictive properties of the model. The solution detailed in Appendix 3 shows that the solution has 27 undetermined parameters and 9 unstable directions. Thus the infra-red fixed point identified previously by ignoring the singlet couplings will *not* be realised. The effect of including the singlet couplings is to destabilise the fixed point in the infra-red direction.

4.5 Example 2: Quark-Line Mixing Model

We next consider a model with mixing along the Q doublet line provided by:

$$n_Q = 9, \tag{80}$$

as in Eq.15. Such a model by itself is not expected to be realistic since it does not account for lepton masses, but it may be regarded as part of a fuller model such as the $n_Q = 9, n_U = 4, n_D = 10, n_E = 8$ example in Tables 3,4.

The superpotential of this example is explicitly:

$$\begin{aligned} W &= h_{33}Q_3U_3^cH_2 + h_{(4)1}Q^{(4)}U_1^cH_2 + h_{(-1)2}Q^{(-1)}U_2^cH_2 + h_{(0)3}Q^{(0)}U_3^cH_2 \\ &+ \sum_{x=-4}^{4} r_{Q^{(x)}}\Phi_Q Q^{(x)}\bar{Q}^{(-x)} \\ &+ s_{Q_1}\theta_Q Q_1\bar{Q}^{(3)} + s_{Q_2}\theta_Q Q_2\bar{Q}^{(-2)} + s_{Q_3}\theta_Q Q_3\bar{Q}^{(-1)} \\ &+ \bar{s}_{Q_2}\bar{\theta}_Q Q_2\bar{Q}^{(0)} + \bar{s}_{Q_3}\bar{\theta}_Q Q_3\bar{Q}^{(1)} \\ &+ \sum_{x=-4}^{3} s_{Q^{(x)}}\theta_Q Q^{(x)}\bar{Q}^{(-x-1)} + \sum_{x=-3}^{4} \bar{s}_{Q^{(x)}}\bar{\theta}_Q Q^{(x)}\bar{Q}^{(-x+1)} \end{aligned} \tag{81}$$

The wavefunction renormalisations for the chiral quarks and leptons and MSSM Higgs doublets are (see Appendix 2):

$$\begin{aligned} N_{Q_3} &= \frac{8}{3}\tilde{\alpha}_3 + \frac{3}{2}\tilde{\alpha}_2 + \frac{1}{18}\tilde{\alpha}_1 - Y^h_{33} - Y^{sQ_3} - Y^{\bar{s}Q_3} \\ N_{Q_2} &= \frac{8}{3}\tilde{\alpha}_3 + \frac{3}{2}\tilde{\alpha}_2 + \frac{1}{18}\tilde{\alpha}_1 - Y^{sQ_2} - Y^{\bar{s}Q_2} \\ N_{Q_1} &= \frac{8}{3}\tilde{\alpha}_3 + \frac{3}{2}\tilde{\alpha}_2 + \frac{1}{18}\tilde{\alpha}_1 - Y^{sQ_1} \\ N_{U_3^c} &= \frac{8}{3}\tilde{\alpha}_3 + \frac{8}{9}\tilde{\alpha}_1 - 2Y^h_{33} - 2Y^h_{(0)3} \\ N_{U_2^c} &= \frac{8}{3}\tilde{\alpha}_3 + \frac{8}{9}\tilde{\alpha}_1 - 2Y^h_{(-1)2} \\ N_{U_1^c} &= \frac{8}{3}\tilde{\alpha}_3 + \frac{8}{9}\tilde{\alpha}_1 - 2Y^h_{(4)1} \\ N_{H_2} &= \frac{3}{2}\tilde{\alpha}_2 + \frac{1}{2}\tilde{\alpha}_1 - 3Y^h_{33} - 3(Y^h_{(4)1} + Y^h_{(-1)2} + Y^h_{(0)3}) \\ N_{Q^{(0)}} &= \frac{8}{3}\tilde{\alpha}_3 + \frac{3}{2}\tilde{\alpha}_2 + \frac{1}{18}\tilde{\alpha}_1 - Y^h_{(0)3} - Y^{rQ_{(0)}} - Y^{sQ_{(0)}} - Y^{\bar{s}Q_{(0)}} \\ N_{Q^{(-1)}} &= \frac{8}{3}\tilde{\alpha}_3 + \frac{3}{2}\tilde{\alpha}_2 + \frac{1}{18}\tilde{\alpha}_1 - Y^h_{(-1)2} - Y^{rQ_{(-1)}} - Y^{sQ_{(-1)}} - Y^{\bar{s}Q_{(-1)}} \\ N_{Q^{(4)}} &= \frac{8}{3}\tilde{\alpha}_3 + \frac{3}{2}\tilde{\alpha}_2 + \frac{1}{18}\tilde{\alpha}_1 - Y^h_{(4)1} - Y^{rQ_{(4)}} - Y^{\bar{s}Q_{(4)}} \\ N_{Q^{(1)}} &= \frac{8}{3}\tilde{\alpha}_3 + \frac{3}{2}\tilde{\alpha}_2 + \frac{1}{18}\tilde{\alpha}_1 - Y^{rQ_{(1)}} - Y^{sQ_{(1)}} \\ N_{Q^{(x\neq 1,0,-1,4)}} &= \frac{8}{3}\tilde{\alpha}_3 + \frac{3}{2}\tilde{\alpha}_2 + \frac{1}{18}\tilde{\alpha}_1 - Y^{rQ_{(x)}} - Y^{sQ_{(x)}} - Y^{\bar{s}Q_{(x)}} \end{aligned}$$

$$
\begin{aligned}
N_{\bar{Q}^{(3)}} &= \frac{8}{3}\tilde{\alpha}_3 + \frac{3}{2}\tilde{\alpha}_2 + \frac{1}{18}\tilde{\alpha}_1 - Y^{^rQ^{(-3)}} - Y^{\bar{s}_Q{}^{(-2)}} - Y^{^sQ^{(-4)}} - Y^{^sQ_1} \\
N_{\bar{Q}^{(-2)}} &= \frac{8}{3}\tilde{\alpha}_3 + \frac{3}{2}\tilde{\alpha}_2 + \frac{1}{18}\tilde{\alpha}_1 - Y^{^rQ^{(2)}} - Y^{\bar{s}_Q{}^{(3)}} - Y^{^sQ^{(1)}} - Y^{^sQ_2} \\
N_{\bar{Q}^{(-1)}} &= \frac{8}{3}\tilde{\alpha}_3 + \frac{3}{2}\tilde{\alpha}_2 + \frac{1}{18}\tilde{\alpha}_1 - Y^{^rQ^{(1)}} - Y^{\bar{s}_Q{}^{(2)}} - Y^{^sQ^{(0)}} - Y^{^sQ_3} \\
N_{\bar{Q}^{(0)}} &= \frac{8}{3}\tilde{\alpha}_3 + \frac{3}{2}\tilde{\alpha}_2 + \frac{1}{18}\tilde{\alpha}_1 - Y^{^rQ^{(0)}} - Y^{\bar{s}_Q{}^{(1)}} - Y^{^sQ^{(-1)}} - Y^{\bar{s}_Q{}_2} \\
N_{\bar{Q}^{(1)}} &= \frac{8}{3}\tilde{\alpha}_3 + \frac{3}{2}\tilde{\alpha}_2 + \frac{1}{18}\tilde{\alpha}_1 - Y^{^rQ^{(-1)}} - Y^{\bar{s}_Q{}^{(0)}} - Y^{^sQ^{(-2)}} - Y^{\bar{s}_Q{}_3} \\
N_{\bar{Q}^{(x\neq 3,-2,-1,0,1)}} &= \frac{8}{3}\tilde{\alpha}_3 + \frac{3}{2}\tilde{\alpha}_2 + \frac{1}{18}\tilde{\alpha}_1 - Y^{^rQ^{(-x)}} - Y^{\bar{s}_Q{}^{(-x+1)}} - Y^{^sQ^{(-x-1)}} \\
N_{\Phi_Q} &= -6\sum_{x=-4}^{4} Y^{^rQ^{(x)}}, \\
N_{\theta_Q} &= -6\sum_{x=-4}^{3} Y^{^sQ^{(x)}} - 6(Y^{^sQ_1} + Y^{^sQ_2} + Y^{^sQ_3}), \\
N_{\bar{\theta}_Q} &= -6\sum_{x=-3}^{4} Y^{\bar{s}_Q{}^{(x)}} - 6(Y^{\bar{s}_Q{}_2} + Y^{\bar{s}_Q{}_3}).
\end{aligned} \tag{82}
$$

The fixed point conditions for the couplings R^h_{33},R^h_{xj}, $R^{^sQ_i}$,$R^{\bar{s}_Q{}_i}$, $R^{^rQ^{(x)}}$, $R^{^sQ^{(x)}}$, $R^{\bar{s}_Q{}^{(x)}}$, are:

$$
\begin{aligned}
N_{Q_3} + N_{U_3^c} + N_{H_2} + \tilde{\alpha}b &= 0 && (83)\\
N_{Q^{(4)}} + N_{U_1^c} + N_{H_2} + \tilde{\alpha}b &= 0 && (84)\\
N_{Q^{(-1)}} + N_{U_2^c} + N_{H_2} + \tilde{\alpha}b &= 0 && (85)\\
N_{Q^{(0)}} + N_{U_3^c} + N_{H_2} + \tilde{\alpha}b &= 0 && (86)\\
N_{\theta_Q} + N_{Q_1} + N_{\bar{Q}^{(3)}} + \tilde{\alpha}b &= 0 && (87)\\
N_{\theta_Q} + N_{Q_2} + N_{\bar{Q}^{(-2)}} + \tilde{\alpha}b &= 0 && (88)\\
N_{\theta_Q} + N_{Q_3} + N_{\bar{Q}^{(-1)}} + \tilde{\alpha}b &= 0 && (89)\\
N_{\bar{\theta}_Q} + N_{Q_2} + N_{\bar{Q}^{(0)}} + \tilde{\alpha}b &= 0 && (90)\\
N_{\bar{\theta}_Q} + N_{Q_3} + N_{\bar{Q}^{(1)}} + \tilde{\alpha}b &= 0 && (91)\\
N_{\Phi_Q} + N_{Q^{(x)}} + N_{\bar{Q}^{(-x)}} + \tilde{\alpha}b &= 0,\ x \in \{-4,\ldots,4\} && (92)\\
N_{\theta_Q} + N_{Q^{(x)}} + N_{\bar{Q}^{(-x-1)}} + \tilde{\alpha}b &= 0,\ x \in \{3,\ldots,-4\} && (93)\\
N_{\bar{\theta}_Q} + N_{Q^{(x)}} + N_{\bar{Q}^{(-x+1)}} + \tilde{\alpha}b &= 0,\ x \in \{4,\ldots,-3\} && (94)
\end{aligned}
$$

If we were to ignore the contribution of the singlet sector then the fixed point equations for the couplings R^h_{33},R^h_{xj}, Eqs.83 and 84, lead to the matrix equation:

$$
\sum_j S_{ij}Y_j = \begin{pmatrix} 6 & 5 & 3 & 3 \\ 5 & 6 & 3 & 3 \\ 3 & 3 & 6 & 3 \\ 3 & 3 & 3 & 6 \end{pmatrix} \begin{pmatrix} Y^h_{33} \\ Y^h_{(0)3} \\ Y^h_{(-1)2} \\ Y^h_{(4)1} \end{pmatrix} = \begin{pmatrix} 1 \\ 1 \\ 1 \\ 1 \end{pmatrix} (r^{QUH_2} + b)\tilde{\alpha} \tag{95}
$$

where $r^{QUH_2} = 88/9$, and we have assumed all the gauge couplings to be equal. Upon inverting the matrix we find,

$$\begin{pmatrix} Y^h_{33} \\ Y^h_{(0)3} \\ Y^h_{(-1)2} \\ Y^h_{(4)1} \end{pmatrix} = \begin{pmatrix} 3 \\ 3 \\ 5 \\ 5 \end{pmatrix} \frac{(r^{QUH_2} + b)}{63} \tilde{\alpha} \tag{96}$$

for the fixed point solutions of the couplings. Note that this solution has a global $SU(2)$ flavour symmetry in the Yukawa couplings of the two lightest families, unlike the Higgs mixing model for example [17]. The reason that it is present in this model is that there is a single Higgs doublet which is common to all the fixed point equations, as compared to the Higgs mixing model where a different Higgs couples in each entry of the Yukawa matrix. When the singlets are included they will explicitly break the global $SU(2)$ flavour symmetry, as we discuss below. Note that in some recent models, such a symmetry is assumed as a starting point [28]. We then checked that the system of RGEs in Eq.59 is infra-red stable in this case by determining the eigenvalues of the matrix S_{ij} in Eq.95. These come out to be $1, 3, 10 + \sqrt{37}, 10 - \sqrt{37}$, so for $b > 0$ (the case considered here), the fixed point is encouragingly infra-red stable in all four independent directions.

Once the singlets are included the above fixed point in Eq.96 will be modified. If we return to Eqs.83-94 we see that there are the same number of equations as unknowns, so the whole system may be regarded as a large matrix which may be inverted along the above lines. From Eqs.83-94 the following relations may be obtained,

$$N_{Q_3} = N_{Q^{(0)}},\ N_{Q_2} = N_{Q^{(1)}},\ N_{Q_1} = N_{Q^{(-4)}}, \tag{97}$$

$$N_{\Phi_Q} = \frac{1}{2}(N_{\theta_Q} + N_{\bar{\theta}_Q}) \tag{98}$$

$$\begin{aligned} N_{\theta_Q} - N_{\Phi_Q} &= N_{Q^{(x+1)}} - N_{Q^{(x)}} = N_{\bar{Q}^{(-x+1)}} - N_{\bar{Q}^{(-x)}} \\ &= N_{Q_2} - N_{Q_3} = N_{U^c_2} - N_{U^c_3} \\ &= \frac{1}{4}(N_{Q_3} - N_{Q_1}) = \frac{1}{4}(N_{U^c_3} - N_{U^c_1}) \\ &= \frac{1}{5}(N_{Q_2} - N_{Q_1}) = \frac{1}{5}(N_{U^c_2} - N_{U^c_1}) \end{aligned} \tag{99}$$

These relations are formally quite model-independent: they apply to any model with $n_Q = 9$ provided Eq.7 holds, regardless of the number of additional states. However the implications of these relations will depend on the particular model under consideration since the wavefunction renormalisations have model dependence. For instance in this particular example, we can immediately see that the previously obtained fixed point based on ignoring the effect of the singlets is not consistent with these equalities. For example it would imply $(N_{U^c_2} - N_{U^c_1}) \propto (5-5) = 0$ and $(N_{U^c_3} - N_{U^c_1}) \propto (9-10) \neq 0$, although the two relations are approximately consistent.

In Appendix 4 we give the fixed point of this example, including the singlets. Out of the 25 independent directions in which the fixed point may attract, 3 are

infra-red unstable and the rest are infra-red stable. We therefore have discovered a saddle point and this will not be realised in nature since the trajectories will actually get further from the fixed point direction as μ, the renormalisation scale decreases. This behaviour is rather similar to that encountered in the Higgs mixing model, and we therefore expect that it may be a general feature of models of this kind, once the singlets are included. Of course, one should in theory check the stability of all the other fixed points involving zeroes in some of the couplings. If one was completely infra-red stable then it would be the fixed point realised by values of the low renormalisation scale couplings. However we shall not pursue this example any further here.

5 Conclusions

We have explored a scenario in which the minimal supersymmetric standard model (MSSM) is valid up to an energy scale of $\sim 10^{16}$ GeV, but that above this scale the theory is supplemented by extra vector-like representations of the gauge group, plus a gauged $U(1)_X$ family symmetry. The basic idea of our approach is that the extra heavy matter above the scale $\sim 10^{16}$ GeV may be used in two different ways: (1) to allow (two-loop) gauge coupling unification at the string scale; (2) to mix with quarks, leptons and Higgs fields via spaghetti diagrams and so lead to phenomenologically acceptable Yukawa textures.

We considered models in which there are enough heavy vector representations to give every effective MSSM-type Yukawa coupling a non-zero value. Using this constraint (detailed by Eqs.24-26), plus the further condition that the mass scale must not be too far below the string scale, we performed a two-loop string gauge unification analysis which yielded 8 models that satisfy these conditions for $\tan\beta = 43$ and 2 for $\tan\beta = 5$ in Tables 3 and 4. For example $n_Q = 9, n_U = 4, n_D = 10, n_E = 8$ (all else zero) satisfies the constraints of string unification independently of $\tan\beta$, and also has enough heavy matter to enable Yukawa textures to be generated via spaghetti diagrams. An example of a different solution is $n_2 = 20, n_S = 24$ where $n_2 = 20$ may be interpreted as being due to $n_{H_1} = 10, n_{H_2} = 10$ as required as in the Higgs mixing model.

Because the dimensionless couplings are of order 1 and because the RG running of the gauge couplings above M_I is steep, one might hope the dimensionless couplings would be forced toward numerical values approximating a fixed point at M_I. This would allow us to make numerical estimates of the values of the fermion masses and mixings at low energy. Motivated by these considerations we constructed the superpotential for a general model involving intermediate matter, and various Standard Model singlets that provide the $U(1)_X$ breaking. We obtained the one-loop RGEs for the general model, and then obtained conditions for stability of the fixed point, showing that the direction of stability in terms of the renormalisation scale depended on the eigenvalues of the coefficient matrix of the fixed point equations.

Having discussed the general case, we then investigated the fixed point of two examples in some detail: a Higgs-line mixing model with $n_{H_1} = 10, n_{H_2} = 10$ and a quark-line mixing model with $n_Q = 9$. Both models have infra-red stable fixed points in the approximation that the couplings involving the singlets are ignored. However when the singlets are included in the analysis we found that the number of undetermined parameters grows (from 3 to 27 in the Higgs-line mixing model, and from 0 to 9 in the Quark-line mixing model) and in addition the fixed point is destabilised in both models. The lesson is clear: it is not in general appropriate to ignore the singlet couplings which must be incorporated fully into the analysis. The most predictive scenario would be one in which the Yukawa couplings depend only upon $\tilde{\alpha}$ in the fixed point solution. It is not yet clear how one could pick a model in which this is likely to be true, or how one could pick a model that possesses a

completely infra-red stable fixed point with all Yukawa couplings non-zero. However it is possible that such a model is contained in the subset of the models in Table 3 which have not all been analysed in detail because of their individual algebraic complexity. The search for a completely realistic model, and the detailed comparison of its low energy predictions to data, is left as the subject of future work. The idea of being able to predict the entire fermion mass spectrum in terms of one or two free parameters is an exciting prospect, and we hope that the general results of the present paper will be helpful in this endeavour.

Acknowledgments

B.A. would like to thank M. Seymour and R. Thorne for discussions on the four-loop QCD beta function. The work of S.F.K. is partially supported by PPARC grant number GR/K55738.

Appendix 1: Two-Loop Renormalisation of MSSM Plus Intermediate States

We derived the following RGEs for the two-loop evolution of the gauge couplings and third family Yukawa couplings in the case of additional intermediate matter from ref. [26]. Note that we have neglected other Yukawa couplings as an approximation. This a good approximation for the bulk of the running which is between M_I and 1 TeV, where the intermediate states have been integrated out of the effective field theory and the effective Yukawa couplings are all much less than 1 apart for $\lambda_{t,b,\tau}$. As we are not considering neutrino masses in this analysis, we assume that there are no neutrino Yukawa couplings in the effective field theory being considered. For now we must assume there are no extra couplings between the superfields of the MSSM and the extra matter for reasons of simplicity and computing time. Naively one might expect these couplings to only change the results slightly because they decouple after less than 2 orders of magnitude in renormalisation running and because they only affect the running of the gauge couplings at the two-loop level. Nonetheless, it should be borne in mind that these couplings could influence the results, particularly in view of the fact that these dimensionless couplings are expected to be of order 1. The equations are valid in the $\overline{DR}$ scheme.

$$
\begin{aligned}
16\pi^2\frac{dg_1}{dt'} &= g_1^3\Big[\frac{33}{5}+\frac{n_Q}{5}+\frac{8n_U}{5}+\frac{2n_D}{5}+\frac{n_S}{10}+\frac{3}{5}n_2+\frac{6}{5}n_E+ \\
&\quad \frac{1}{16\pi^2}\Big(-\frac{26}{5}\lambda_t^2-\frac{14}{5}\lambda_b^2-\frac{18}{5}\lambda_\tau^2+\frac{36}{25}g_1^2\Big(\frac{199}{25}+\frac{n_Q}{108}+\frac{n_2}{4}+ \\
&\quad \frac{2n_D+32n_U}{27}+\frac{2n_S}{43}+2n_E\Big)+g_2^2\Big(\frac{27}{5}+\frac{3n_Q}{5}+\frac{9n_2}{5}\Big)+ \\
&\quad g_3^2\frac{16}{5}\Big(\frac{88}{5}+\frac{n_Q}{3}+\frac{n_S}{6}+\frac{8n_U+2n_D}{3}\Big)\Big)\Big] \\
16\pi^2\frac{dg_2}{dt'} &= g_2^3\Big[1+3n_Q+n_2+\frac{1}{16\pi^2}\Big(-6\lambda_t^2-6\lambda_b^2-2\lambda_\tau^2+g_2^2\,(25+ \\
&\quad 7(3n_Q+n_2))+\frac{3}{10}g_1^2\Big(6+\frac{2n_Q}{3}+2n_2\Big)+8g_3^2\,(2n_Q+3)\Big)\Big] \\
16\pi^2\frac{dg_3}{dt'} &= g_3^3\Big[-3+2n_Q+n_U+n_D+n_S+\frac{1}{16\pi^2}\Big(-4\lambda_t^2-4\lambda_b^2+g_3^2\,(14+ \\
&\quad \frac{68}{3}n_Q+\frac{34}{3}n_S+\frac{34}{3}n_U+\frac{34}{3}n_D\Big)+g_1^2\Big(\frac{11}{5}+\frac{2}{15}n_Q+\frac{16}{15}n_U+ \\
&\quad \frac{4}{15}n_D+\frac{2}{30}n_S\Big)+g_2^2\,(9+6n_Q)\Big)\Big] \\
16\pi^2\frac{d\lambda_t}{dt'} &= \lambda_t\Big[6\lambda_t^2+\lambda_b^2-\frac{13}{15}g_1^2-3g_2^2-\frac{16}{3}g_3^2+\frac{1}{16\pi^2}\Big(g_1^4\frac{2743}{450}+ \\
&\quad g_2^4\frac{15}{2}-g_3^4\frac{16}{9}+\frac{136}{45}g_1^2g_3^2+g_1^2g_2^2+8g_2^2g_3^2+\lambda_t^2\Big(\frac{6}{5}g_1^2+ \\
&\quad 6g_2^2+16g_3^2\Big)+\frac{2}{5}\lambda_b^2g_1^2-22\lambda_t^4-5\lambda_b^2\lambda_t^2-5\lambda_b^4-\lambda_b^2\lambda_\tau^2\Big)\Big]
\end{aligned}
$$

$$
\begin{aligned}
16\pi^2\frac{d\lambda_b}{dt'} &= \lambda_b\Big[6\lambda_b^2+\lambda_t^2+\lambda_\tau^2-\frac{7}{15}g_1^2-3g_2^2-\frac{16}{3}g_3^2+\frac{1}{16\pi^2}\Big(\frac{287}{90}g_1^4+ \\
&\quad \frac{15}{2}g_2^4-\frac{17}{9}g_3^4+g_1^2g_2^2+\frac{8}{9}g_1^2g_3^2+8g_2^2g_3^2+\frac{4}{5}\lambda_t^2g_1^2+\lambda_b^2\Big(\frac{2}{5}g_1^2+ \\
&\quad 6g_2^2+16g_3^2\Big)+\frac{6}{5}\lambda_\tau^2g_1^2-22\lambda_b^2-5\lambda_t^2\lambda_b^2-3\lambda_b^2\lambda_\tau^2-3\lambda_\tau^4-5\lambda_t^4\Big)\Big] \\
16\pi^2\frac{d\lambda_\tau}{dt'} &= \lambda_\tau\Big[4\lambda_\tau^2+3\lambda_b^2-\frac{9}{5}g_1^2-3g_2^2+\frac{1}{16\pi^2}\Big(\frac{27}{2}g_1^4+\frac{15}{2}g_2^4+\frac{9}{2}g_1^2g_2^2 \\
&\quad +\lambda_b^2\Big(16g_3^2-\frac{2}{5}g_1^2\Big)+\lambda_\tau^2\Big(\frac{6}{5}g_1^2+6g_2^2\Big)-3\lambda_b^2\lambda_t^2-9\lambda_b^4 \\
&\quad -9\lambda_b^2\lambda_\tau^2-10\lambda_\tau^4\Big)\Big] \qquad (100)
\end{aligned}
$$

where $t'=\ln\mu$ and μ is the $\overline{DR}$ renormalisation scale.

We now detail the matching conditions between the $\overline{DR}$ and the $\overline{MS}$ schemes [27]:

$$
\begin{aligned}
g_2^{\overline{DR}}(m_t) &= \frac{g_2^{\overline{MS}}(m_t)}{1-g_2^{\overline{MS}}(m_t)^2/48\pi^2} \\
g_3^{\overline{DR}}(m_t) &= \frac{g_3^{\overline{MS}}(m_t)}{1-g_3^{\overline{MS}}(m_t)^2/32\pi^2} \\
\lambda_{t,b}^{\overline{DR}}(m_t) &= \frac{\lambda_{t,b}^{\overline{MS}}(m_t)}{1+g_3^{\overline{MS}}(m_t)^2/12\pi^2-3g_2^{\overline{MS}}(m_t)^2/128\pi^2}, \qquad (101)
\end{aligned}
$$

where the superscripts denote what scheme the quantity is evaluated in. To a good approximation, $g_1^{\overline{DR}}=g_1^{\overline{MS}}$ and $\lambda_\tau^{\overline{DR}}=\lambda_\tau^{\overline{MS}}$. Our running value of m_t is determined by

$$
m_t^{phys}=m_t(m_t)(1+\frac{g_3^2(m_t)}{3\pi^2}) \qquad (102)
$$

where m_t^{phys} is the value extracted from experiment. For $m_t^{phys}=180$ GeV [21] and central values of $\alpha_S(M_Z)$, we obtain $m_t(m_t)=166$ GeV.

Appendix 2: One-loop wavefunction renormalisation of the general model

Here we give the wavefunction renormalisation contributions to the RGEs for the general model in Eq.56. In the following equations for the wavefunction renormalisation of N_i, all sums are intended to be over couplings that multiply the field i in Eq.56:

$$
\begin{aligned}
N_{Q_i} &= \frac{8}{3}\tilde{\alpha}_3+\frac{3}{2}\tilde{\alpha}_2+\frac{1}{18}\tilde{\alpha}_1-\sum_j Y_{ij}^h-\sum_j Y_{ij}^k-\sum_y Y_{iy}^h-\sum_y Y_{iy}^k-Y^{sQ_i}-Y^{\bar{s}Q_i} \\
N_{U_j^c} &= \frac{8}{3}\tilde{\alpha}_3+\frac{8}{9}\tilde{\alpha}_1-2\sum_i Y_{ij}^h-2\sum_x Y_{xj}^h-Y^{sU_j}-Y^{\bar{s}U_j}
\end{aligned}
$$

$$
\begin{aligned}
N_{D_j^c} &= \frac{8}{3}\tilde{\alpha}_3 + \frac{2}{9}\tilde{\alpha}_1 - 2\sum_i Y_{ij}^k - 2\sum_x Y_{xj}^k - Y^{s_{D_j^c}} - Y^{\bar{s}_{D_j^c}} \\
N_{L_i} &= \frac{3}{2}\tilde{\alpha}_2 + \frac{1}{2}\tilde{\alpha}_1 - \sum_j Y_{ij}^l - \sum_y Y_{iy}^l - Y^{s_{L_i}} - Y^{\bar{s}_{L_i}} \\
N_{E_j^c} &= 2\tilde{\alpha}_1 - 2\sum_i Y_{ij}^l - 2\sum_x Y_{xj}^l - Y^{s_{E_j^c}} - Y^{\bar{s}_{E_j^c}}
\end{aligned} \tag{103}
$$

The wavefunction renormalisations for the vector states are:

$$
\begin{aligned}
N_{Q^{(x)}} &= \frac{8}{3}\tilde{\alpha}_3 + \frac{3}{2}\tilde{\alpha}_2 + \frac{1}{18}\tilde{\alpha}_1 \\
&\quad - \sum_j Y_{xj}^h - \sum_j Y_{xj}^k - \sum_y Y_{xy}^h - \sum_y Y_{xy}^k - Y^{r_{Q_x}} - Y^{s_{Q^{(x)}}} - Y^{\bar{s}_{Q^{(x)}}} \\
N_{U^{c(y)}} &= \frac{8}{3}\tilde{\alpha}_3 + \frac{8}{9}\tilde{\alpha}_1 - 2\sum_i Y_{iy}^h - 2\sum_x Y_{xy}^h - Y^{r_{U^{c(y)}}} - Y^{s_{U^{c(y)}}} - Y^{\bar{s}_{U^{c(y)}}} \\
N_{D^{c(y)}} &= \frac{8}{3}\tilde{\alpha}_3 + \frac{2}{9}\tilde{\alpha}_1 - 2\sum_i Y_{iy}^k - 2\sum_x Y_{xy}^k - Y^{r_{D^{c(y)}}} - Y^{s_{D^{c(y)}}} - Y^{\bar{s}_{D^{c(y)}}} \\
N_{L^{(x)}} &= \frac{3}{2}\tilde{\alpha}_2 + \frac{1}{2}\tilde{\alpha}_1 - \sum_j Y_{xj}^l - \sum_y Y_{xy}^l - Y^{r_{L_x}} - Y^{s_{L^{(x)}}} - Y^{\bar{s}_{L^{(x)}}} \\
N_{E^{c(y)}} &= 2\tilde{\alpha}_1 - 2\sum_i Y_{iy}^l - 2\sum_x Y_{xy}^l - Y^{r_{E^{c(y)}}} - Y^{s_{E^{c(y)}}} - Y^{\bar{s}_{E^{c(y)}}} \\
N_{H_1^{(z)}} &= \frac{3}{2}\tilde{\alpha}_2 + \frac{1}{2}\tilde{\alpha}_1 - 3\sum_{ij} Y_{ij}^k - \sum_{ij} Y_{ij}^l - 3\sum_{iy} Y_{iy}^k - \sum_{iy} Y_{iy}^l \\
&\quad - 3\sum_{xj} Y_{xj}^k - \sum_{xj} Y_{xj}^l - 3\sum_{xy} Y_{xy}^k - \sum_{xy} Y_{xy}^l - Y^{r_{H_1^{(z)}}} - Y^{s_{H_1^{(z)}}} - Y^{\bar{s}_{H_1^{(z)}}} \\
N_{H_2^{(z)}} &= \frac{3}{2}\tilde{\alpha}_2 + \frac{1}{2}\tilde{\alpha}_1 \\
&\quad - 3\sum_{ij} Y_{ij}^h - 3\sum_{iy} Y_{iy}^h - 3\sum_{xj} Y_{xj}^h - 3\sum_{xy} Y_{xy}^h - Y^{r_{H_2^{(z)}}} - Y^{s_{H_2^{(z)}}} - Y^{\bar{s}_{H_2^{(z)}}} \\
N_{\bar{Q}^{(-x)}} &= \frac{8}{3}\tilde{\alpha}_3 + \frac{3}{2}\tilde{\alpha}_2 + \frac{1}{18}\tilde{\alpha}_1 \\
&\quad - \sum_y Y_{xy}^{\bar{h}} - \sum_y Y_{xy}^{\bar{k}} - Y^{r_{Q_x}} - Y^{\bar{s}_{Q^{(x+1)}}} - Y^{s_{Q^{(x-1)}}} - Y^{s_{Q_i}} - Y^{\bar{s}_{Q_i}} \\
N_{\bar{U}^{c(-y)}} &= \frac{8}{3}\tilde{\alpha}_3 + \frac{8}{9}\tilde{\alpha}_1 - 2\sum_x Y_{xy}^{\bar{h}} - Y^{r_{U^{c(y)}}} - Y^{\bar{s}_{U^{c(y+1)}}} - Y^{s_{U^{c(y-1)}}} - Y^{s_{U_j}} - Y^{\bar{s}_{U_j}} \\
N_{\bar{D}^{c(-y)}} &= \frac{8}{3}\tilde{\alpha}_3 + \frac{2}{9}\tilde{\alpha}_1 - 2\sum_x Y_{xy}^{\bar{k}} - Y^{r_{D^{c(y)}}} - Y^{\bar{s}_{D^{c(y+1)}}} - Y^{s_{D^{c(y-1)}}} - Y^{s_{D_j}} - Y^{\bar{s}_{D_j}} \\
N_{\bar{L}^{(-x)}} &= \frac{3}{2}\tilde{\alpha}_2 + \frac{1}{2}\tilde{\alpha}_1 - \sum_y Y_{xy}^{\bar{l}} - Y^{r_{L_x}} - Y^{\bar{s}_{L_{x+1}}} - Y^{s_{L^{(x-1)}}} - Y^{s_{L_j}} - Y^{\bar{s}_{L_j}} \\
N_{\bar{E}^{c(-y)}} &= 2\tilde{\alpha}_1 - 2\sum_x Y_{xy}^{\bar{l}} - Y^{r_{E^{c(y)}}} - Y^{\bar{s}_{E^{c(y+1)}}} - Y^{s_{E^{c(y-1)}}} - Y^{s_{E_j}} - Y^{\bar{s}_{E_j}} \\
N_{\bar{H}_1^{(-z)}} &= \frac{3}{2}\tilde{\alpha}_2 + \frac{1}{2}\tilde{\alpha}_1 - 3\sum_{xy} Y_{xy}^{\bar{k}} - \sum_{xy} Y_{xy}^{\bar{l}} - Y^{r_{H_1^{(z)}}} - Y^{\bar{s}_{H_1^{(z+1)}}} - Y^{s_{H_1^{(z-1)}}}
\end{aligned}
$$

$$N_{\bar{H}_2^{(z)}} = \frac{3}{2}\tilde{\alpha}_2 + \frac{1}{2}\tilde{\alpha}_1 - 3\sum_{xy} Y^{\bar{h}}_{xy} - Y^{r_{H_2^{(z)}}} - Y^{\bar{s}_{H_2^{(z+1)}}} - Y^{s_{H_2^{(z-1)}}} \quad (104)$$

The wavefunction contributions for the singlets are:

$$\begin{aligned}
N_{\Phi_Q} &= -6\sum_x Y^{rQ^x},\ N_{\Phi_{U^c}} = -3\sum_y Y^{rU^{cy}},\ N_{\Phi_{D^c}} = -3\sum_y Y^{rD^{cy}} \\
N_{\Phi_L} &= -2\sum_x Y^{rL^x},\ N_{\Phi_{E^c}} = -\sum_y Y^{rE^{cy}}, \\
N_{\Phi_{H_1}} &= -2\sum_z Y^{rH_1^z},\ N_{\Phi_{H_2}} = -2\sum_z Y^{rH_2^z} \\
N_{\theta_Q} &= -6\sum_x Y^{sQ^x} - 6\sum_i Y^{sQ_i},\ N_{\theta_{U^c}} = -3\sum_y Y^{sU^{cy}} - 3\sum_j Y^{sU_j}, \\
N_{\theta_{D^c}} &= -3\sum_y Y^{sD^{cy}} - 3\sum_j Y^{sD_j}, \\
N_{\theta_L} &= -2\sum_x Y^{sL^x} - 2\sum_i Y^{sL_i},\ N_{\theta_{E^c}} = -\sum_y Y^{sE^{cy}} - \sum_j Y^{sE_j}, \\
N_{\theta_{H_1}} &= -2\sum_z Y^{sH_1^z},\ N_{\theta_{H_2}} = -2\sum_z Y^{sH_2^z} \\
N_{\bar{\theta}_Q} &= -6\sum_x Y^{\bar{s}Q^x} - 6\sum_i Y^{\bar{s}Q_i},\ N_{\bar{\theta}_{U^c}} = -3\sum_y Y^{\bar{s}U^{cy}} - 3\sum_j Y^{\bar{s}U_j}, \\
N_{\bar{\theta}_{D^c}} &= -3\sum_y Y^{\bar{s}D^{cy}} - 3\sum_j Y^{\bar{s}D_j}, \\
N_{\bar{\theta}_L} &= -2\sum_x Y^{\bar{s}L^x} - 2\sum_i Y^{\bar{s}L_i},\ N_{\bar{\theta}_{E^c}} = -\sum_y Y^{\bar{s}E^{cy}} - \sum_j Y^{\bar{s}E_j}, \\
N_{\bar{\theta}_{H_1}} &= -2\sum_z Y^{\bar{s}H_1^z},\ N_{\bar{\theta}_{H_2}} = -2\sum_z Y^{\bar{s}H_2^z}
\end{aligned} \quad (105)$$

Appendix 3: Fixed point solution of the Higgs Mixing model including singlets

For the Higgs Mixing model corresponding to the superpotential in Eq.70 with symmetric inputs for the l, h, k matrices at a high scale but including the singlet couplings, we now present the solutions to the fixed point equations:

$$\begin{aligned}
R^{h_{22}} &= \frac{583}{216} - R^{h_{21}} + \frac{25\ b}{112} - R^{h_{32}} \\
R^{l_{11}} &= -\frac{25\ b}{84} - \frac{5}{2} + 2R^{l_{32}} + R^{l_{33}} + R^{l_{22}} \\
R^{s_{H_2^{(-2)}}} &= \frac{3\ b}{28} + \frac{1}{2} - R^{s_{H_2^{(-1)}}} - R^{r_{H_2^{(-1)}}} \\
R^{r_{H_2^{(-2)}}} &= R^{s_{H_2^{(-1)}}} + R^{r_{H_2^{(-1)}}} \\
R^{s_{H_1^{(0)}}} &= R^{\bar{s}_{H_1^{(1)}}} \\
R^{\bar{s}_{H_1^{(0)}}} &= \frac{3\ b}{28} + \frac{1}{2} - R^{\bar{s}_{H_1^{(1)}}} - R^{r_{H_1^{(0)}}}
\end{aligned}$$

$$
\begin{aligned}
R^{s}{}_{H_1^{(-1)}} &= \frac{3\,b}{28} + \frac{1}{2} - R^{\bar{s}}{}_{H_1^{(1)}} - R^{r}{}_{H_1^{(0)}} \\
\bar{s}_{H_1^{(-1)}} &= -R^{r}{}_{H_1^{(-1)}} + R^{\bar{s}}{}_{H_1^{(1)}} + R^{r}{}_{H_1^{(0)}} \\
R^{r}{}_{H_1^{(-2)}} &= \frac{3\,b}{28} + \frac{1}{2} + R^{r}{}_{H_1^{(-1)}} - R^{\bar{s}}{}_{H_1^{(1)}} - R^{r}{}_{H_1^{(0)}} \\
R^{s}{}_{H_1^{(-2)}} &= -R^{r}{}_{H_1^{(-1)}} + R^{\bar{s}}{}_{H_1^{(1)}} + R^{r}{}_{H_1^{(0)}} \\
R^{s}{}_{H_2^{(0)}} &= R^{\bar{s}}{}_{H_2^{(1)}} \\
R^{s}{}_{H_1^{(1)}} &= \frac{3\,b}{28} + \frac{1}{2} - R^{r}{}_{H_1^{(1)}} - R^{\bar{s}}{}_{H_1^{(1)}} \\
R^{\bar{s}}{}_{H_1^{(2)}} &= \frac{3\,b}{28} + \frac{1}{2} - R^{r}{}_{H_1^{(1)}} - R^{\bar{s}}{}_{H_1^{(1)}} \\
R^{r}{}_{H_2^{(1)}} &= R^{\bar{s}}{}_{H_2^{(3)}} + R^{r}{}_{H_2^{(2)}} - R^{\bar{s}}{}_{H_2^{(1)}} \\
R^{s}{}_{H_2^{(1)}} &= \frac{3\,b}{28} + \frac{1}{2} - R^{\bar{s}}{}_{H_2^{(3)}} - R^{r}{}_{H_2^{(2)}} \\
R^{\bar{s}}{}_{H_2^{(2)}} &= \frac{3\,b}{28} + \frac{1}{2} - R^{\bar{s}}{}_{H_2^{(3)}} - R^{r}{}_{H_2^{(2)}} \\
R^{r}{}_{H_2^{(0)}} &= \frac{3\,b}{28} + \frac{1}{2} - R^{s}{}_{H_2^{(-1)}} - R^{\bar{s}}{}_{H_2^{(1)}} \\
\bar{s}_{H_2^{(-1)}} &= \frac{3\,b}{28} + \frac{1}{2} - R^{s}{}_{H_2^{(-1)}} - R^{r}{}_{H_2^{(-1)}} \\
R^{\bar{s}}{}_{H_2^{(0)}} &= R^{s}{}_{H_2^{(-1)}} \\
R^{\bar{s}}{}_{H_1^{(3)}} &= R^{s}{}_{H_1^{(2)}} \\
R^{r}{}_{H_1^{(2)}} &= R^{r}{}_{H_1^{(1)}} - R^{s}{}_{H_1^{(2)}} + R^{\bar{s}}{}_{H_1^{(1)}} \\
R^{s}{}_{H_2^{(2)}} &= R^{\bar{s}}{}_{H_2^{(3)}} \\
R^{h_{11}} &= \frac{25\,b}{112} + \frac{583}{216} - R^{h_{31}} - R^{h_{21}} \\
R^{h_{31}} &= R^{h_{31}} \\
R^{k_{31}} &= \frac{463}{216} + \frac{25\,b}{112} - R^{k_{11}} - R^{k_{21}} \\
R^{l_{31}} &= \frac{5}{2} - R^{l_{32}} - R^{l_{33}} + \frac{25\,b}{84} \\
R^{l_{21}} &= \frac{25\,b}{84} + \frac{5}{2} - R^{l_{32}} - R^{l_{22}} \\
s_{H_2^{(7)}} &= R^{\bar{s}}{}_{H_2^{(8)}} \\
R^{r}{}_{H_2^{(8)}} &= \frac{3\,b}{28} + \frac{1}{2} - R^{\bar{s}}{}_{H_2^{(8)}} \\
R^{\bar{s}}{}_{H_2^{(6)}} &= R^{s}{}_{H_2^{(5)}} \\
R^{r}{}_{H_1^{(8)}} &= \frac{1}{2} + \frac{3\,b}{28} - R^{\bar{s}}{}_{H_1^{(8)}} \\
R^{s}{}_{H_1^{(7)}} &= R^{\bar{s}}{}_{H_1^{(8)}}
\end{aligned}
$$

$$
\begin{aligned}
R^{r}{}_{H_1^{(3)}} &= \frac{b}{28}+\frac{1}{6}-R^{r}{}_{H_1^{(1)}}-R^{r}{}_{H_1^{(-1)}}-R^{r}{}_{H_1^{(5)}}+R^{\bar{s}}{}_{H_1^{(8)}}+R^{\bar{s}}{}_{H_1^{(7)}}\\
R^{\bar{s}}{}_{H_1^{(4)}} &= \frac{b}{14}+\frac{1}{3}+R^{r}{}_{H_1^{(1)}}-R^{s}{}_{H_1^{(2)}}+R^{r}{}_{H_1^{(-1)}}+R^{r}{}_{H_1^{(5)}}-R^{\bar{s}}{}_{H_1^{(8)}}-R^{\bar{s}}{}_{H_1^{(7)}}\\
R^{\bar{s}}{}_{H_1^{(5)}} &= \frac{3\,b}{28}+\frac{1}{2}-R^{s}{}_{H_1^{(5)}}-R^{r}{}_{H_1^{(5)}}\\
R^{s}{}_{H_1^{(4)}} &= \frac{3\,b}{28}+\frac{1}{2}-R^{s}{}_{H_1^{(5)}}-R^{r}{}_{H_1^{(5)}}\\
R^{s}{}_{H_1^{(3)}} &= \frac{b}{14}+\frac{1}{3}+R^{r}{}_{H_1^{(1)}}-R^{s}{}_{H_1^{(2)}}+R^{r}{}_{H_1^{(-1)}}+R^{r}{}_{H_1^{(5)}}-R^{\bar{s}}{}_{H_1^{(8)}}-R^{\bar{s}}{}_{H_1^{(7)}}\\
R^{k_{32}} &= -R^{k_{33}}+R^{k_{11}}+R^{k_{21}}\\
R^{h_{33}} &= \frac{25\,b}{112}+\frac{583}{216}-R^{h_{32}}-R^{h_{31}}\\
R^{k_{22}} &= \frac{25\,b}{112}+\frac{463}{216}-2R^{k_{21}}-R^{k_{11}}+R^{k_{33}}\\
R^{s}{}_{H_2^{(6)}} &= R^{\bar{s}}{}_{H_2^{(7)}}\\
R^{\bar{s}}{}_{H_2^{(4)}} &= \frac{b}{14}+\frac{1}{3}+R^{r}{}_{H_2^{(2)}}+R^{r}{}_{H_2^{(-1)}}-R^{\bar{s}}{}_{H_2^{(1)}}-R^{\bar{s}}{}_{H_2^{(8)}}+R^{r}{}_{H_2^{(5)}}-R^{\bar{s}}{}_{H_2^{(7)}}\\
R^{s}{}_{H_2^{(3)}} &= \frac{b}{14}+\frac{1}{3}+R^{r}{}_{H_2^{(2)}}+R^{r}{}_{H_2^{(-1)}}-R^{\bar{s}}{}_{H_2^{(1)}}-R^{\bar{s}}{}_{H_2^{(8)}}+R^{r}{}_{H_2^{(5)}}-R^{\bar{s}}{}_{H_2^{(7)}}\\
R^{s}{}_{H_1^{(6)}} &= R^{\bar{s}}{}_{H_1^{(7)}}\\
R^{r}{}_{H_1^{(7)}} &= \frac{3\,b}{28}+\frac{1}{2}-R^{\bar{s}}{}_{H_1^{(8)}}-R^{\bar{s}}{}_{H_1^{(7)}}\\
R^{\bar{s}}{}_{H_1^{(6)}} &= R^{s}{}_{H_1^{(5)}}\\
R^{r}{}_{H_1^{(6)}} &= \frac{3\,b}{28}+\frac{1}{2}-R^{s}{}_{H_1^{(5)}}-R^{\bar{s}}{}_{H_1^{(7)}}\\
R^{r}{}_{H_1^{(4)}} &= -\frac{b}{14}-\frac{1}{3}+R^{\bar{s}}{}_{H_1^{(8)}}+R^{\bar{s}}{}_{H_1^{(7)}}-R^{r}{}_{H_1^{(1)}}+s_{H_1^{(2)}}-R^{r}{}_{H_1^{(-1)}}+R^{s}{}_{H_1^{(5)}}\\
R^{r}{}_{H_2^{(3)}} &= \frac{b}{28}+\frac{1}{6}-R^{\bar{s}}{}_{H_2^{(3)}}-R^{r}{}_{H_2^{(2)}}-R^{r}{}_{H_2^{(-1)}}+R^{\bar{s}}{}_{H_2^{(1)}}+R^{\bar{s}}{}_{H_2^{(8)}}-R^{r}{}_{H_2^{(5)}}+R^{\bar{s}}{}_{H_2^{(7)}}\\
R^{s}{}_{H_2^{(4)}} &= \frac{3\,b}{28}+\frac{1}{2}-R^{s}{}_{H_2^{(5)}}-R^{r}{}_{H_2^{(5)}}\\
R^{\bar{s}}{}_{H_2^{(5)}} &= \frac{3\,b}{28}+\frac{1}{2}-R^{s}{}_{H_2^{(5)}}-R^{r}{}_{H_2^{(5)}}\\
R^{r}{}_{H_2^{(4)}} &= -\frac{b}{14}-\frac{1}{3}-R^{r}{}_{H_2^{(2)}}-R^{r}{}_{H_2^{(-1)}}+R^{\bar{s}}{}_{H_2^{(1)}}+R^{\bar{s}}{}_{H_2^{(8)}}+R^{s}{}_{H_2^{(5)}}+R^{\bar{s}}{}_{H_2^{(7)}}\\
R^{r}{}_{H_2^{(6)}} &= \frac{3\,b}{28}+\frac{1}{2}-R^{s}{}_{H_2^{(5)}}-R^{\bar{s}}{}_{H_2^{(7)}}\\
R^{r}{}_{H_2^{(7)}} &= \frac{3\,b}{28}+\frac{1}{2}-R^{\bar{s}}{}_{H_2^{(8)}}-R^{\bar{s}}{}_{H_2^{(7)}}. \qquad (106)
\end{aligned}
$$

The eigenvalues of the matrix S are

$$
\begin{aligned}
\bar{\lambda}_i &= \{-6.0,-12.0,-4.0,-6.0,-2.0,-6.0,-9.0,-5.0,-4.0,26.6\\
&\quad 21.2,20.2,5.68,5.36,4.83,4.32,3.72,3.18,3.92,3.68,2.69
\end{aligned}
$$

$$3.31, 2.0, 0.317, 2.08, 2.32, 0.633, 2.81, 1.67, 1.17, 2.28, 26.6$$
$$21.2, 20.2, 5.68, 5.36, 4.83, 4.32, 3.72, 3.18, 2.69, 2.0, 2.08$$
$$2.32, 3.92, 0.317, 3.68, 0.633, 3.31, 1.17, 2.81, 1.67, 2.28$$
$$0, 0, 0, 0, 0, 0, 0, 0, 0, 0, 0, 0, 0, 0, 0, 0, 0, 0, 0, 0, 0, 0, 0, 0, 0, 0, 0, 0, 0, 0\} \quad (107)$$

to 3 significant figure accuracy.

Appendix 4: Fixed point solution of Quark-line mixing model including singlets

On solving the fixed point Eqs.83-94 including the singlet sector, we obtain

$$\begin{aligned}
R^{s}{}_{Q^{(-1)}} &= -\frac{95\,b}{1078} - \frac{13865}{14553} - R^{r}{}_{Q^{(-1)}} - R^{s}{}_{Q^{(-2)}} \\
R^{\bar{s}}{}_{Q^{(-1)}} &= \frac{115}{441} + \frac{3\,b}{98} + R^{s}{}_{Q^{(-2)}} \\
R^{\bar{s}}{}_{Q_2} &= -\frac{117\,b}{539} - \frac{10930}{4851} - R^{r}{}_{Q^{(0)}} + R^{r}{}_{Q^{(-1)}} + R^{s}{}_{Q^{(-2)}} \\
R^{\bar{s}}{}_{Q_3} &= \frac{575}{1323} + \frac{5\,b}{98} - R^{\bar{s}}{}_{Q^{(0)}} - R^{r}{}_{Q^{(-1)}} - R^{s}{}_{Q^{(-2)}} \\
R^{s}{}_{Q_2} &= \frac{267\,b}{1078} + \frac{1355}{539} + R^{r}{}_{Q^{(0)}} - R^{r}{}_{Q^{(-1)}} - R^{s}{}_{Q^{(-2)}} \\
R^{s}{}_{Q_3} &= -\frac{5465}{4851} + R^{h}{}_{(0)3} - \frac{117\,b}{1078} + R^{\bar{s}}{}_{Q^{(0)}} + R^{r}{}_{Q^{(-1)}} + R^{s}{}_{Q^{(-2)}} \\
R^{s}{}_{Q^{(3)}} &= \frac{5465}{4851} + \frac{117\,b}{1078} + R^{\bar{s}}{}_{Q^{(4)}} \\
R^{\bar{s}}{}_{Q^{(3)}} &= -\frac{6\,b}{77} - \frac{200}{231} - R^{\bar{s}}{}_{Q^{(4)}} - R^{r}{}_{Q^{(3)}} \\
R^{r}{}_{Q^{(4)}} &= -\frac{10070}{14553} - \frac{31\,b}{539} - R^{\bar{s}}{}_{Q^{(4)}} \\
R^{s}{}_{Q^{(2)}} &= \frac{5\,b}{98} + \frac{575}{1323} - R^{\bar{s}}{}_{Q^{(4)}} - R^{r}{}_{Q^{(3)}} \\
R^{h}{}_{(-1)2} &= \frac{13865}{14553} + \frac{95\,b}{1078} \\
R^{h}{}_{(4)1} &= \frac{13865}{14553} + \frac{95\,b}{1078} \\
R^{s}{}_{Q_1} &= \frac{3\,b}{98} + \frac{115}{441} \\
R^{s}{}_{Q^{(0)}} &= \frac{115}{441} - R^{h}{}_{(0)3} - R^{r}{}_{Q^{(0)}} - R^{\bar{s}}{}_{Q^{(0)}} + \frac{3\,b}{98} \\
R^{h}{}_{33} &= -R^{h}{}_{(0)3} + \frac{13865}{14553} + \frac{95\,b}{1078} \\
R^{\bar{s}}{}_{Q^{(1)}} &= \frac{192\,b}{539} + \frac{17660}{4851}
\end{aligned}$$

$$
\begin{aligned}
R^{r}{}_{Q^{(2)}} &= \frac{115}{1323} + \frac{b}{98} - R^{r}{}_{Q^{(0)}} + R^{\bar{s}}{}_{Q^{(4)}} - R^{r}{}_{Q^{(-3)}} + R^{s}{}_{Q^{(-2)}} \\
R^{s}{}_{Q^{(1)}} &= -\frac{139\,b}{1078} - \frac{18925}{14553} + R^{r}{}_{Q^{(-1)}} + R^{r}{}_{Q^{(3)}} + R^{r}{}_{Q^{(-3)}} \\
R^{r}{}_{Q^{(1)}} &= \frac{86\,b}{539} + \frac{22720}{14553} - R^{r}{}_{Q^{(-1)}} - R^{r}{}_{Q^{(3)}} - R^{r}{}_{Q^{(-3)}} \\
R^{\bar{s}}{}_{Q^{(-3)}} &= \frac{b}{98} + \frac{115}{1323} - R^{r}{}_{Q^{(-3)}} + R^{s}{}_{Q^{(-2)}} + R^{r}{}_{Q^{(-2)}} \\
R^{r}{}_{Q^{(-4)}} &= \frac{460}{1323} + \frac{2\,b}{49} + R^{r}{}_{Q^{(-3)}} - R^{s}{}_{Q^{(-2)}} - R^{r}{}_{Q^{(-2)}} \\
R^{s}{}_{Q^{(-3)}} &= \frac{b}{49} + \frac{230}{1323} - R^{s}{}_{Q^{(-2)}} - R^{r}{}_{Q^{(-2)}} \\
R^{\bar{s}}{}_{Q^{(-2)}} &= \frac{3\,b}{98} + \frac{115}{441} - R^{s}{}_{Q^{(-2)}} - R^{r}{}_{Q^{(-2)}} \\
R^{s}{}_{Q^{(-4)}} &= -\frac{b}{98} - \frac{115}{1323} - R^{r}{}_{Q^{(-3)}} + R^{s}{}_{Q^{(-2)}} + R^{r}{}_{Q^{(-2)}} \\
R^{\bar{s}}{}_{Q^{(2)}} &= -\frac{3\,b}{98} - \frac{115}{441} + R^{r}{}_{Q^{(0)}} + R^{r}{}_{Q^{(3)}} + R^{r}{}_{Q^{(-3)}} - R^{s}{}_{Q^{(-2)}}. \qquad (108)
\end{aligned}
$$

Eq.108 shows that in fact 25 out of the 34 variables are constrained. This must mean that within Eqs.83-94, 9 of the 34 constraints exhibit degeneracy. Even given this proviso, we appear to have greatly increased the predictivity of the model. Unfortunately though, there is a problem with the stability properties of the above fixed point. When the eigenvalues of the matrix corresponding to the generalisation of S_{ij} are determined, we find they are:

$$
\begin{aligned}
\bar{\lambda}_i = \{&66.8, 48.0, 16.2, 15.0, 3.68, 4.53 + 0.233i, 4.53 - 0.233i, -2.63, 4.19, 3.36, \\
&3.23, 2.71 + 0.122i, 2.71 - 0.122i, 2.33, 1.82, 1.08 + 0.562i, 1.08 - 0.562i, \\
&1.34 + 0.182i, 1.34 - 0.182i, -0.477, 0.885, 0.275 + 0.119i, 0.275 - 0.119i, \\
&0.392, -0.195, 0, 0, 0, 0, 0, 0, 0, 0, 0\}. \qquad (109)
\end{aligned}
$$

References

[1] U.Amaldi et al., Phys. Rev. **D36** (1987) 1385;
P.Langacker and M.Luo, Phys. Rev. **D44** (1991) 817;
J.Ellis,S.Kelley and D.V.Nanopoulos, Phys. Lett. **B249** (1990) 441;
Nucl. Phys. **B373** (1992) 55;
U.Amaldi, W. de Boer and H.Fustenau, Phys. Lett. **B260** (1991) 447;
C. Giunti, C.W. Kim and U.W. Lee, Mod. Phys. Lett. **A6** (1991) 1745;
H.Arason et al., Phys. Rev. **D46** (1992) 3945;
F.Anselmo, L.Cifarelli, A.Peterman and A.Zichichi, Nuovo Cimento 105A (1992) 1179;
P.Langacker and N.Polonski, Phys. Rev. **D47** (1993) 4028;
A.E.Faraggi and B.Grinstein, Nucl. Phys. **B422** (1994) 3.

[2] K. Dienes, `hep-th/9602045`, Phys. Rep. (to appear).

[3] L. Hall and S. Raby, Phys. Rev. **D51** (1995) 6524.

[4] C.Bachas and C.Fabre, `hep-ph/9505318`;
A.A.Maslikov, I.A.Naumov and G.G.Volkov, `hep-ph/9512429`.

[5] D. Lewellen, Nucl. Phys. **B337** (1990) 61;
A. Font, L. Ibanez and F. Quevedo, Nucl. Phys. **B345** (1990) 389;
S. Chaudhuri, S-w Chung and J. Lykken, `hep-ph/9405374`;
G.Aldazabal, A.Font, L.E.Ibanez and A.M.Uranga, Nucl. Phys. **B452** (1995) 3;
I.A.Antionadis, J.Ellis, J.Hagelin and D.V.Nanopoulos, Phys. Lett. **B194** (1987) 231;
I.A.Antionadis, J.Ellis, J.Hagelin and D.V.Nanopoulos, Phys. Lett. **B231** (1989) 65;
I.A.Antionadis and G.K.Leontaris, Phys. Lett. **B216** (1989) 33;
I.A.Antionadis, G.K.Leontaris and J.Rizos, Phys. Lett. **B245** (1990) 161.

[6] J.Ellis, S. Kelley and D.V.Nanopoulos, Phys. Lett. **B249** (1990) 241;
C.Bachas, C.Fabre and T.Yanagida, NSF-ITP-95-129, CPTH-S379.1095, `hep-th/951004`;
P.H.Chankowski, Z.Pluciennik, S. Pokorski and C.E.Vayonakis, Phys. Lett. **B358** (1995) 264;
A. de la Macorra, Phys. Lett. **B341** (1994) 31;
H.P.Nilles, TUM-HEP-234/96, SFB-375/28.

[7] V.Kaplunovsky, Nucl. Phys. **B307** (1988) 145.

[8] L.E.Ibanez, Phys. Lett. **B318** (1993) 73.

[9] Choi and Kiwoon, Phys. Rev. **D37** (1988) 1564;
P. Mayr, H.P.Nilles and S.Steinberger, Phys. Lett, **B317** (1993) 53;
D.Bailin and A.Love, Phys. Lett. **B292** (1992) 315;

E. Halyo, hep-ph/9509323;
V.Kaplunovsky, Nucl. Phys. **B307** (1988) 145;
I.A.Antionadis, J.Ellis, R.Lacaze and D.V.Nanopoulos, Phys. Lett. **B268** (1991) 188;
J.P.Deredinger, S.Ferrara, C.Kounnas and F.Zwirner, Phys. Lett. **B271** (1991) 307;
J.P.Deredinger, S.Ferrara, C.Kounnas and F.Zwirner, Nucl. Phys. **B372** (1992) 145;
L.Ibanez, D.Lust and G.G.Ross, Phys. Lett. **B272** (1991) 251;
L.Dixon, V.Kaplunovsky and J.Louis, Nucl. Phys. **B335** (1991) 649;
I.A.Antionadis, E.Gava, K.S.Narain and T.Taylor, Nucl. Phys. **B407** (1993) 706;
E.Kiritsis and C.Kounnass, Nucl. Phys. **B442** (1995) 472;
V.Kaplunovsky and J.Louis, Nucl. Phys. **B444** (1995) 191;
P.M.Petropoulos and J.Rizos, hep-th/9601037.

[10] K.R.Dienes and A.E.Faraggi, Phys. Rev. Lett. **75** (1995) 2646;
K.R.Dienes and A.E.Faraggi, Nucl. Phys. **B457** (1995) 409.

[11] J.Ellis, S.Kelley and D.V.Nanopoulos, Phys. Lett. **B260** (1991) 131;
I. Antoniadis, J. Ellis, S. Kelley and D.V. Nanopoulos, Phys. Lett. **B272** (1991) 31;
D.Bailin and A.Love, Phys. Lett. **B280** (1992) 26;
D.Bailin and A.Love, Mod. Phys. Lett. **A7** (1992) 1485;
J.Lopez and D.V.Nanopoulos, DOE-ER-40717-20, CTP-TAMU-45-95, ACT-16-95, hep-ph/9511426;
A.E.Faraggi, Phys. Lett. **B302** (1993) 202;
J.Lopez, D.V.Nanopoulos and K.Yuan, Nucl. Phys. **B335** (1990) 347;
M.K.Gaillard and R.Xiu, Phys. Lett. **B296** (1992) 71;
I.A.Antionadis and K.Benakli, Phys. Lett. **B295** (1992) 219;
R.Xiu, Phys. Rev. **D49** (1994) 6656.

[12] S.Martin and P.Ramond, Phys. Rev. **D51** (1995) 6515.

[13] S.F.King and B.C.Allanach, Nucl. Phys. **B473** (1996) 3.

[14] B.Pendleton and G.Ross, Phys. Lett.**B98** (1981) 291.

[15] C.Hill, Phys. Rev. **D24** (1981) 691.

[16] M.Lanzagorta and G. Ross, Phys. Lett. **B349** (1995) 319.

[17] G.G.Ross, Phys. Lett. **B364** (1995) 216.

[18] L.Ibanez and G.Ross, Phys. Lett. **B332** (1994) 100.

[19] C. D. Froggatt and H. B. Nielsen, Nucl. Phys. **B147** (1979) 277.

[20] S. Chang, C. Coriano and A.E.Farraggi, Nucl. Phys. **B477** (1996) 65.

[21] Review of Particle Physics, Phys. Rev. **D54** (1996) 1.

[22] S. G. Gorishny, A. L. Kataev, S. A. Larin, and L. R. Surgaladze, Mod. Phys. Lett. **A 5** (1990) 2703;
O. V. Tarasov, A. A. Vladimirov, and A. Yu. Zharkov, Phys. Lett. **B 93** (1980) 429;
S. G. Korishny, A. L. Kataev, S. A. Larin, and P. Lett., Phys. Lett. **B 135** (1984) 457.

[23] T. van Ritbergen, J.A.M.Vermaseren and S.A.Larin, UM-TH-97-01, NIHHEF-97-001, hep-ph/9701390.

[24] B.C. Allanach and S.F. King, Phys. Lett. **B328** (1994) 360.

[25] I. Jack and D.R.T. Jones, Phys. Lett. **B349** (1995) 294.

[26] S.P. Martin and M.T. Vaughn, Phys. Rev. **D 50** (1994) 2282.

[27] S.P. Martin and M.T.Vaughn, Phys. Lett. **B318** (1993) 331.

[28] R. Barbieri, L. J. Hall, S. Raby, A. Romanino, hep-ph/9610449; R. Barbieri, L. J. Hall, hep-ph/9605224; R. Barbieri, G. Dvali, L. J. Hall, Phys.Lett. **B377** (1996) 76.